Electronic Supplementary Material (ESI) for Dalton Transactions.

Supporting Information

Investigating the chemical sensitivity of melting in zeolitic imidazolate frameworks

Alice M. Bumstead,[a] Michael F. Thorne,[a] Adam F. Sapnik,[a] Celia Castillo-Blas,[a] Giulio I. Lampronti,[b] and Thomas D. Bennett *[a]

Contact Email: tdb35@cam.ac.uk

[a.] Department of Materials Science and Metallurgy, University of Cambridge, Cambridge, CB3 0FS, UK.

[b.] Department of Earth Sciences, University of Cambridge, Cambridge, CB2 3EQ, UK.

Contents

Figures

Tables

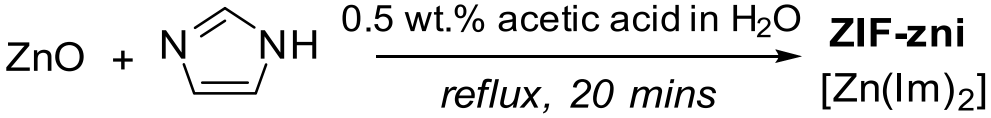

Figure S1: Reaction scheme for synthesis of ZIF-zni. Based on method reported by Schubert *et al.*[1]

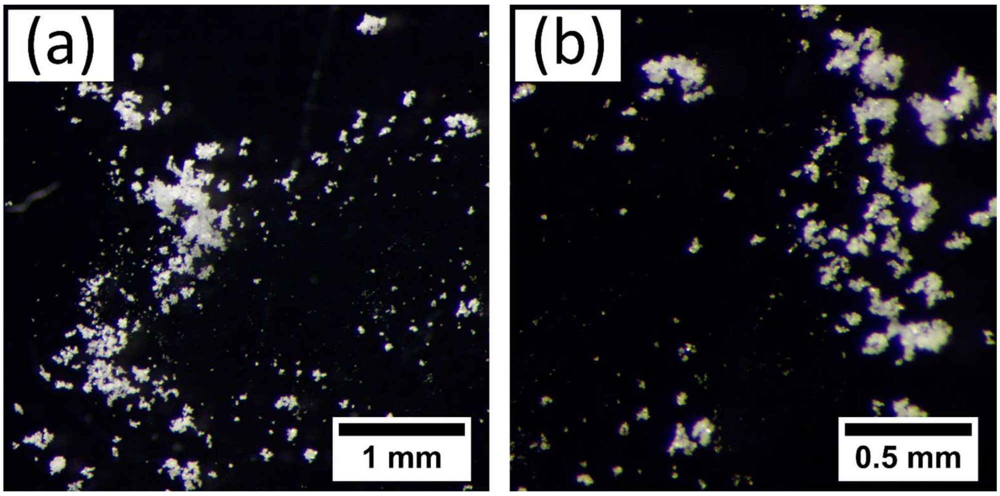

Figure S2: Optical microscope images of ZIF-zni powder. Scale bars were added using ImageJ 1.52.[2]

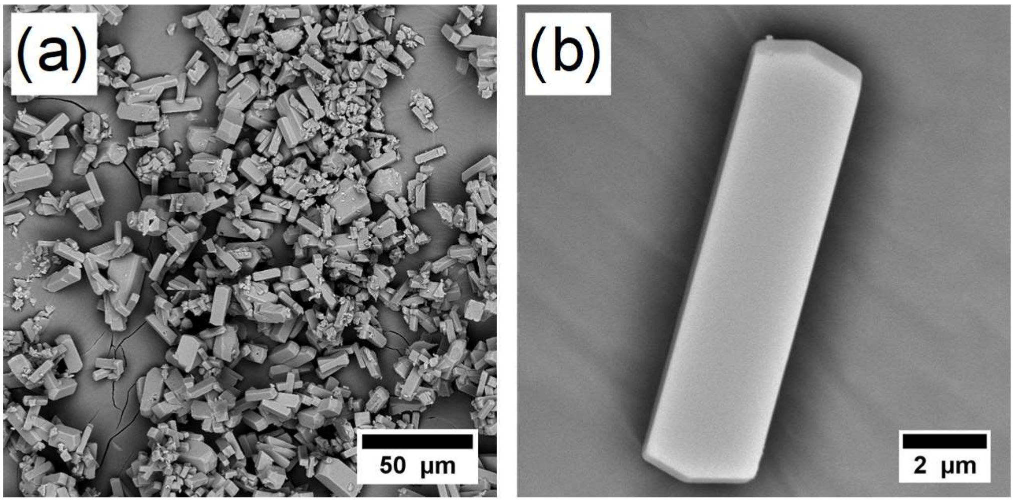

Figure S3: Scanning electron microscope images of ZIF-zni powder. Scale bars were added using ImageJ 1.52.[2]

Table S1: Data from Pawley refinement of ZIF-zni

R_{wp}	**Space Group**	**Lattice Parameters**	**Reported Parameters for ZIF-zni**[3]
7.606	$I4_1cd$	a = 23.5091(8) Å	a = 23.5028(4) Å
		c = 12.4617(5) Å	c = 12.4607(3) Å
		α = β = γ = 90 °	α = β = γ = 90 °

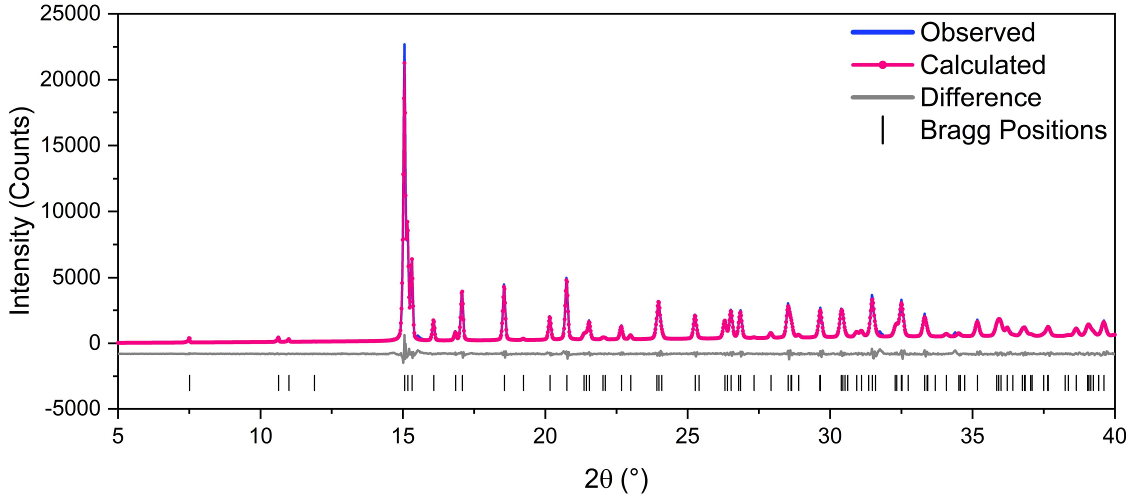

Figure S4: Pawley refinement of powder X-ray diffraction (PXRD) data of activated ZIF-zni powder. Initial parameters were obtained from the reported CIF for ZIF-zni.[3] Conversion of .raw files to .xy files was performed using PowDLL and all powder refinements were performed using TOPAS-Academic Version 6.[4,5] Difference curve and Bragg positions are offset on the y axis for clarity.

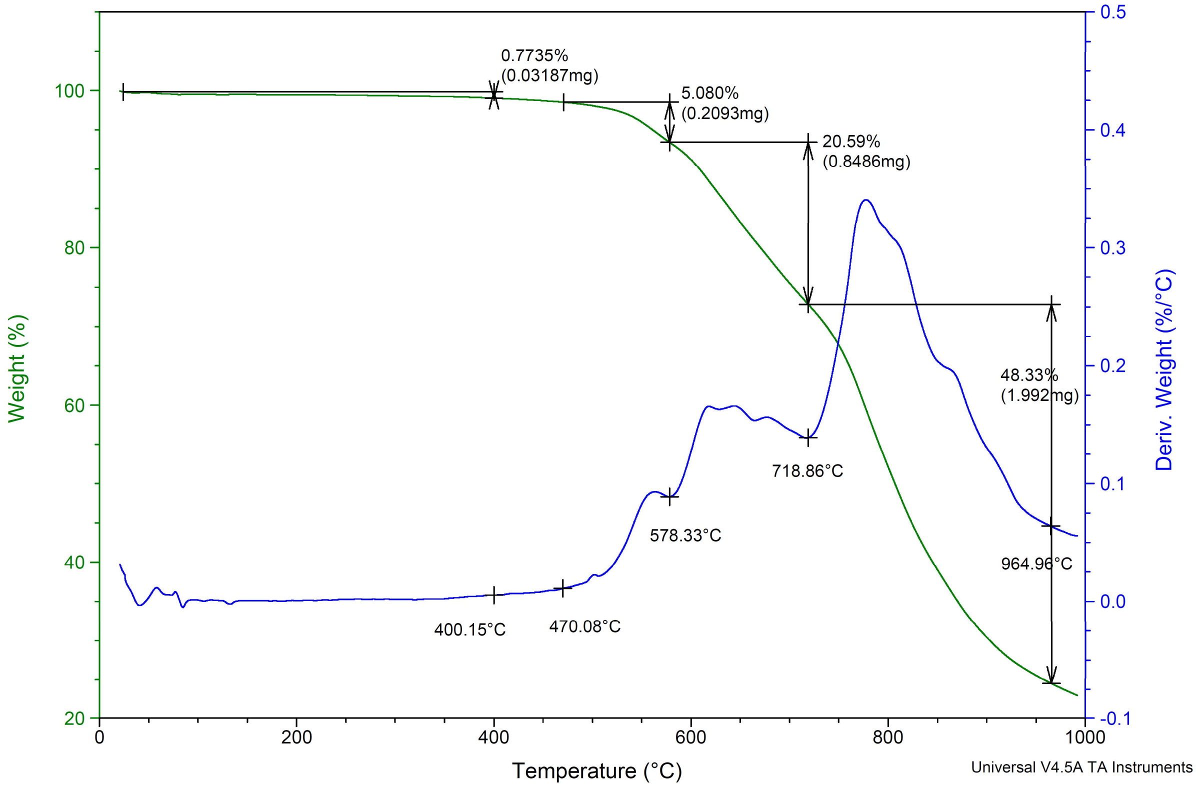

Figure S5: Thermogravimetric analysis (TGA) of ZIF-zni powder heated at 10 °C min^{-1} up to 1000 °C under argon. Weight (%) curve shown in green and derivative weight (%/°C) curve shown in blue. Data collected on a TA Instruments Q600 SDT (SDT – Simultaneous Differential scanning calorimetry and Thermogravimetric analysis). All data analysis was performed using the TA Instruments Universal Analysis software package.[6]

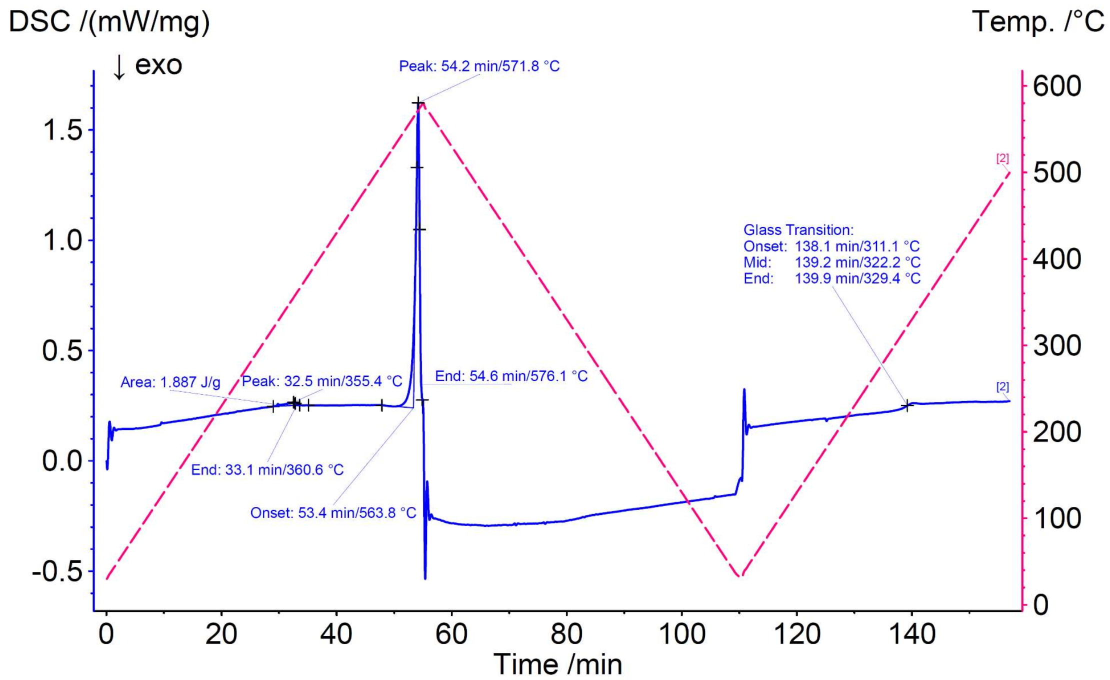

Figure S6: Differential scanning calorimetry (DSC) of ZIF-zni powder heated to 580 °C, cooled to 30 °C and heated to 500 °C at 10 °C min^{-1} under argon. DSC curve shown in blue and temperature trace shown in pink. Data collected on a Netzsch DSC 214 Polyma Instrument. All data analysis was performed using the Netzsch Proteus® software package.[7]

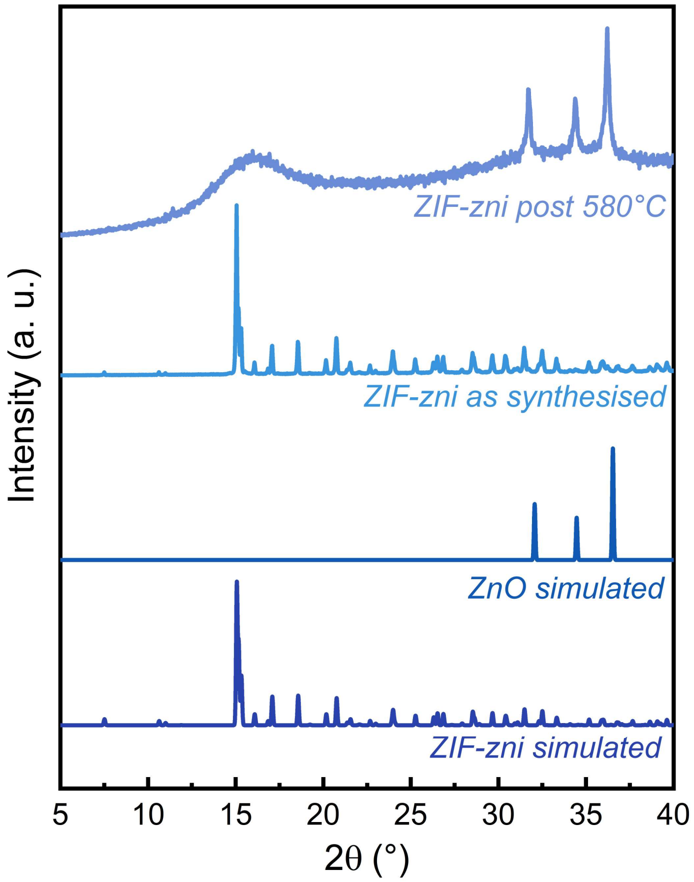

Figure S7: PXRD patterns between 5-40° of as prepared ZIF-zni (light blue) and a_gZIF-zni (lilac) (after heating to 580 °C) compared to the simulated diffraction pattern of ZIF-zni (dark blue) obtained from a previously published CIF[3] and ZnO (mid blue). a_gZIF-zni did not display reflections associated with the ZIF-zni crystal structure after heating although reflections corresponding to ZnO were observed.

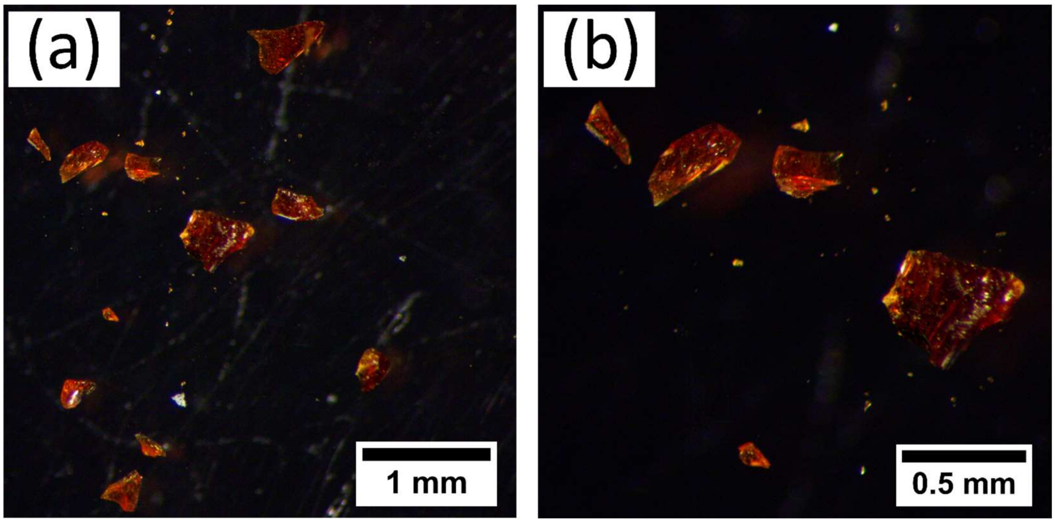

Figure S8: Optical microscope images of ZIF-zni after heating to 580 °C. Clear evidence of flow and glass formation had occurred, although decomposition related discolouration was also observed.

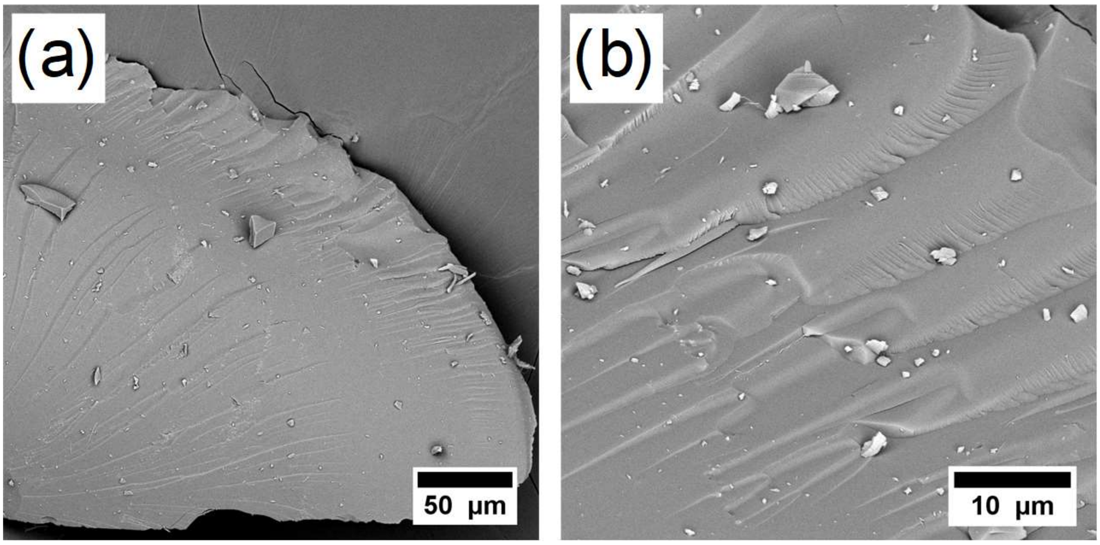

Figure S9: Scanning electron microscope images of ZIF-zni after heating to 580 °C. Clear evidence of particle coalescence and flow related striations were visible, further indicating that glass formation had occurred.

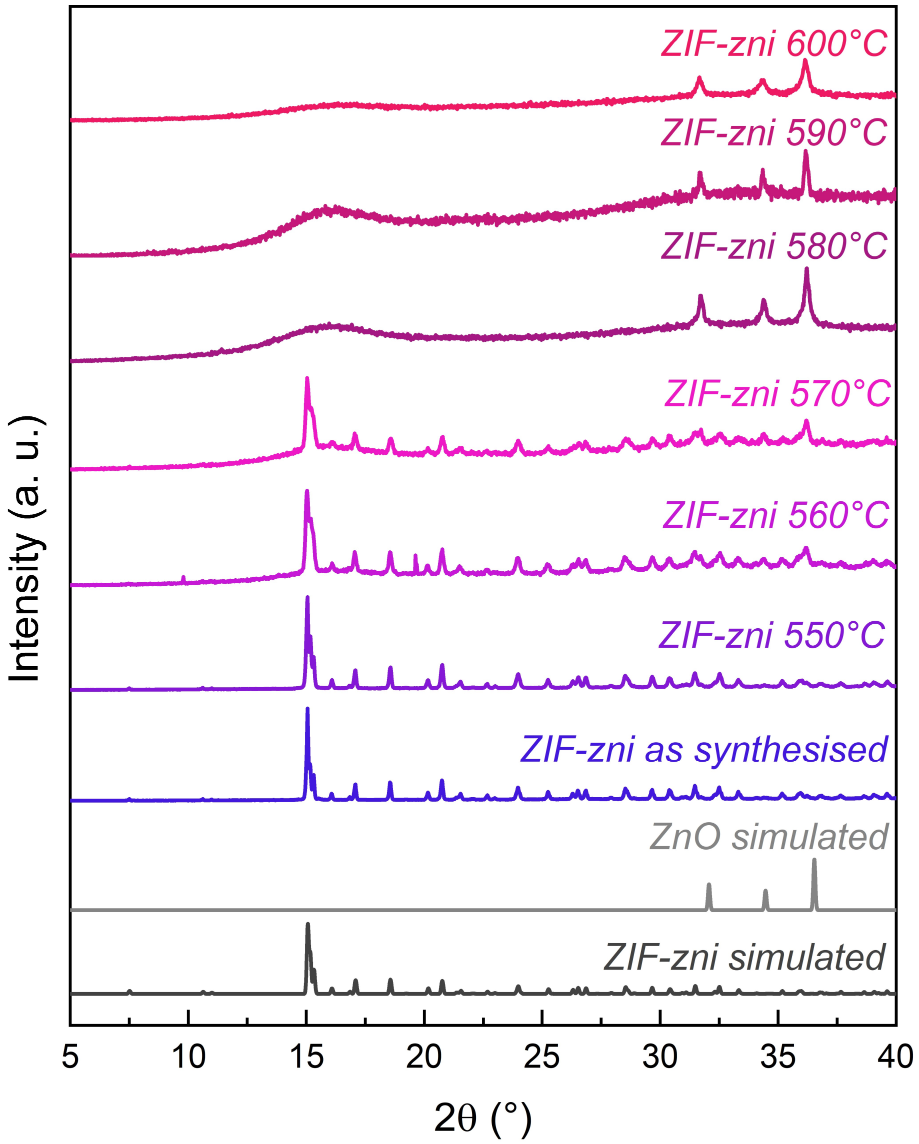

Figure S10: PXRD patterns between 5-40° of as prepared ZIF-zni (blue) and ZIF-zni heated to 550-600 °C (purple to red) compared to the simulated diffraction pattern of ZIF-zni (dark grey) and ZnO (light grey). Evidence of ZnO is observed as low as 560 °C suggesting that it is not possible to prepare a_gZIF-zni without ZnO contamination.

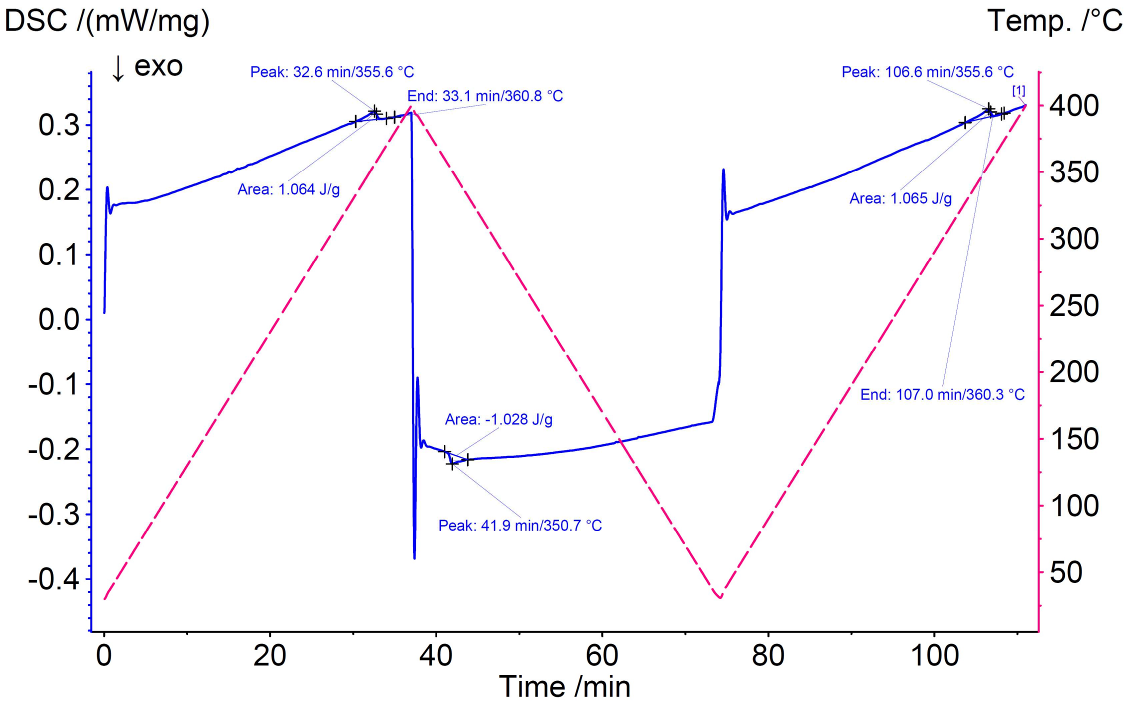

Figure S11: DSC of ZIF-zni powder heated to 400 °C, cooled to 30 °C and heated to 400 °C at 10 °C min^{-1} under argon. DSC curve shown in blue and temperature trace shown in pink. Time is shown on the x-axis.

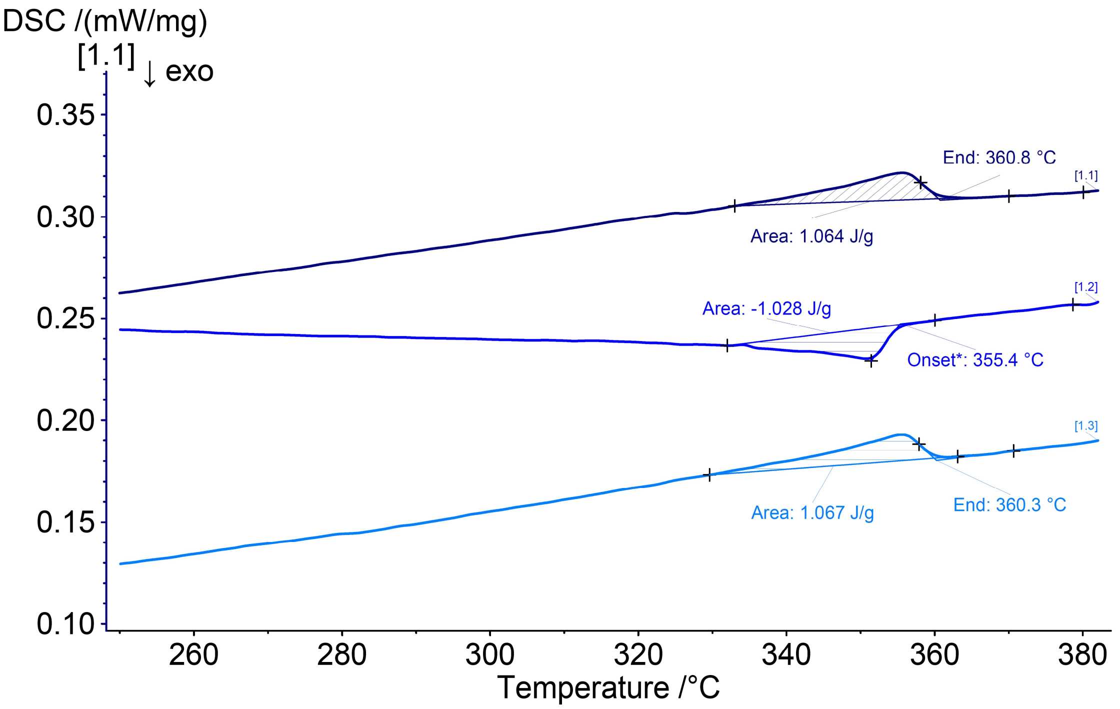

Figure S12: DSC of ZIF-zni powder heated to 400 °C, cooled to 30 °C and heated to 400 °C at 10 °C min^{-1} under argon. Temperature is shown on the x-axis. DSC traces are separated into segments: 1st upscan – navy, downscan – blue, 2nd upscan – light blue. DSC segments are offset on the y-axis for clarity.

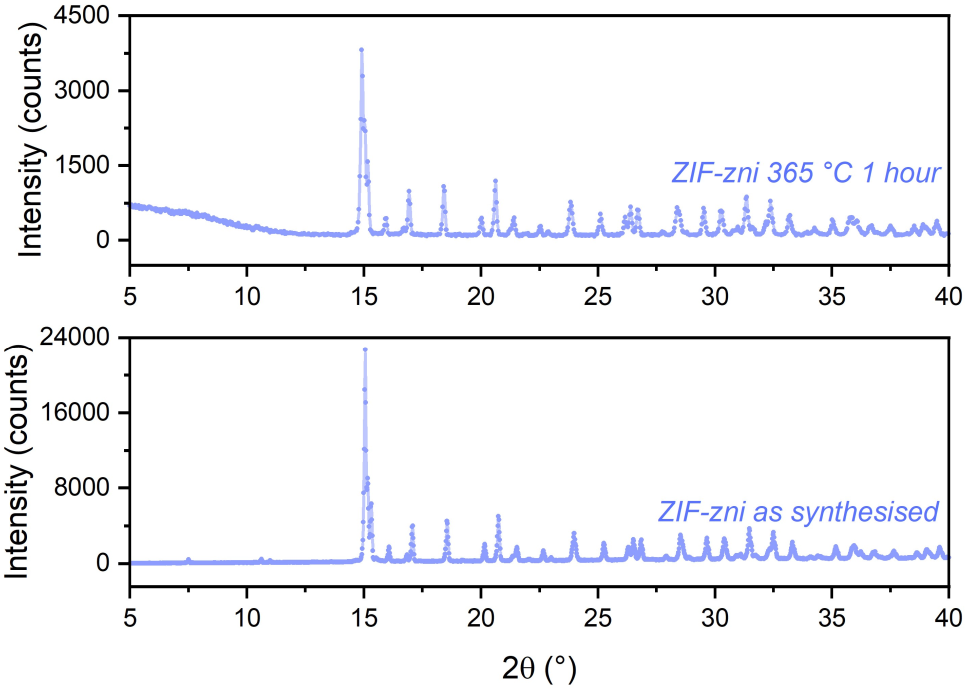

Figure S13: PXRD patterns between 5-40° of as prepared ZIF-zni (bottom pane) and ZIF-zni heated to 365 °C for 1 hour (top pane). No discernible difference in the number or position of reflections was observed, with the only noticeable change being a drop in the overall intensity after heating.

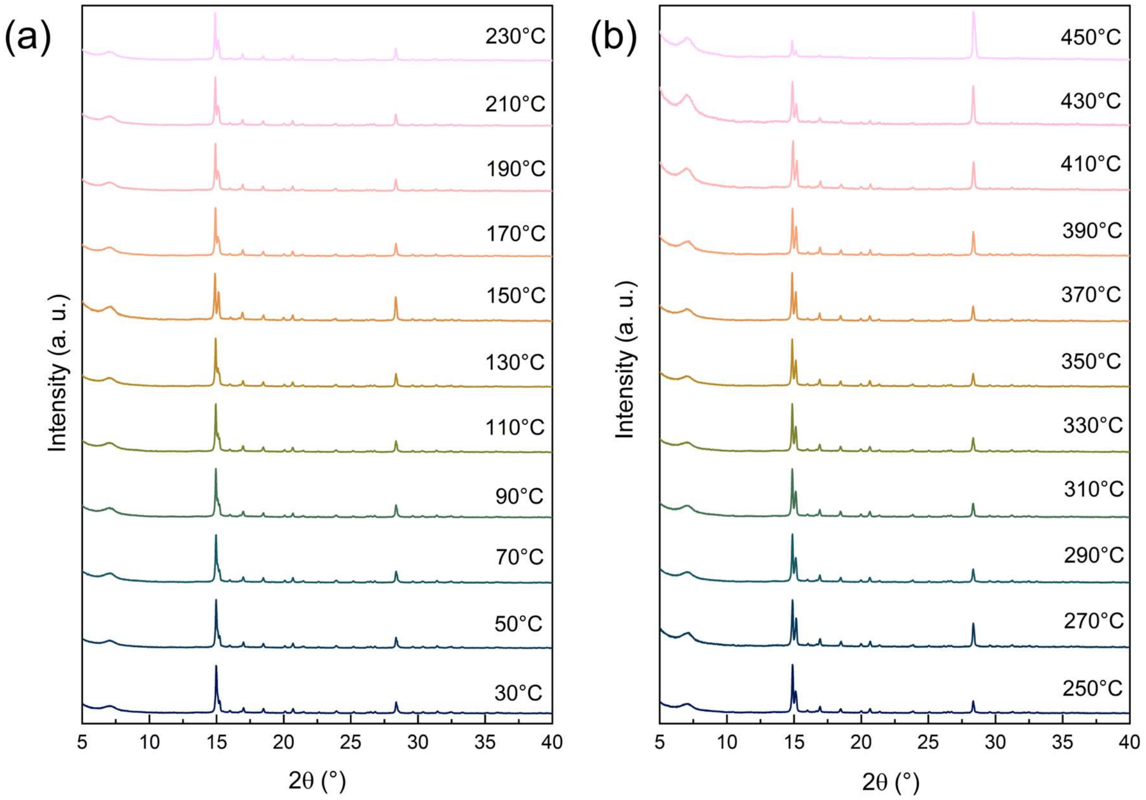

Figure S14: Variable temperature powder X-ray diffraction (VTPXRD) data for ZIF-zni between 30 and 230 °C (a) and 250 to 450 °C (b). Data were collected at 20 °C intervals from 30 °C to 450 °C and a silicon standard was used as a reference. The broad peak at 7° is from the alumina sample holder.

Table S2: Lattice parameters and errors obtained from VTPXRD measurement of ZIF-zni

Temp. (°C)	**Rwp**	**χ^2**	***a* (Å)**	**esd (Å)**	***c* (Å)**	**esd (Å)**	**V (Å^3)**	**esd (Å^3)**
30	9.579	2.212	23.520	0.002	12.463	0.002	6894.18	1.55
50	9.157	2.108	23.533	0.002	12.463	0.001	6901.97	1.48
70	8.949	2.005	23.552	0.002	12.462	0.001	6912.42	1.53
90	8.976	1.985	23.563	0.002	12.458	0.001	6916.71	1.54
110	9.374	2.078	23.576	0.002	12.457	0.001	6923.78	1.67
130	9.026	2.013	23.595	0.002	12.457	0.001	6934.78	1.62
150	9.224	2.053	23.601	0.003	12.452	0.001	6935.74	1.72
170	8.920	1.982	23.615	0.002	12.451	0.001	6943.08	1.63
190	9.134	2.013	23.624	0.002	12.447	0.001	6946.79	1.64
210	8.965	1.978	23.639	0.002	12.446	0.001	6955.22	1.65
230	9.439	2.103	23.650	0.003	12.443	0.001	6959.99	1.69
250	9.899	2.214	23.662	0.003	12.442	0.002	6966.2	1.70
270	9.164	2.037	23.675	0.002	12.440	0.001	6972.39	1.57
290	8.895	1.965	23.687	0.002	12.439	0.001	6979.49	1.54
310	8.750	1.944	23.694	0.002	12.436	0.001	6981.81	1.56
330	9.287	2.052	23.698	0.002	12.434	0.001	6982.89	1.61
350	9.203	2.000	23.705	0.002	12.432	0.001	6985.72	1.69
370	9.063	1.969	23.716	0.002	12.432	0.001	6992.47	1.60
390	8.580	1.850	23.725	0.003	12.433	0.002	6998.35	1.87
410	7.727	1.583	23.709	0.003	12.419	0.002	6981.05	2.18
430	7.503	1.450	23.725	0.005	12.423	0.003	6993.05	3.65
450	11.972	2.337	23.878	0.015	12.501	0.008	7127.28	10.15

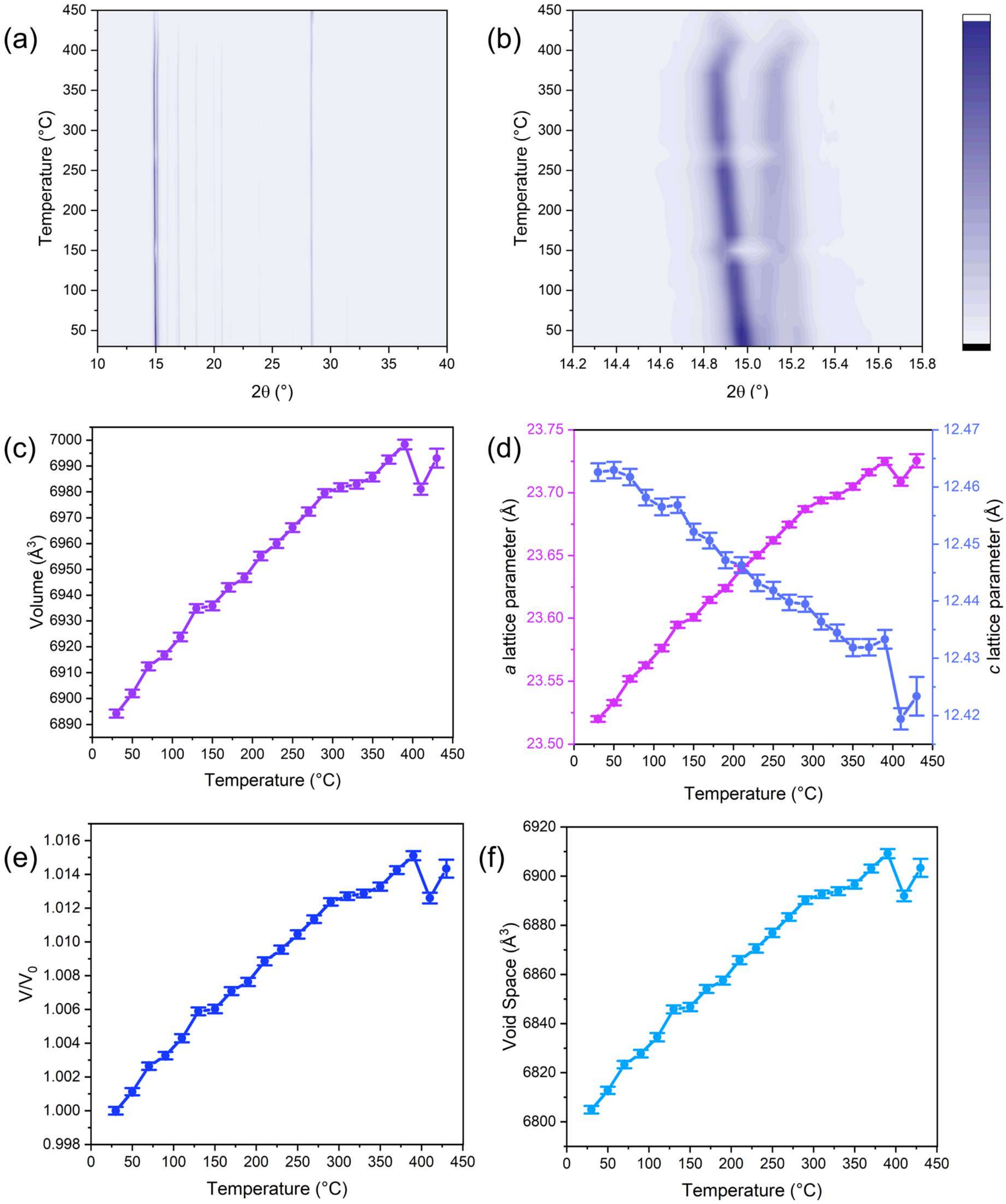

Figure S15: (a) Contour plot of VTPXRD data collected on ZIF-zni, plotted between 10-40° 2θ. No obvious changes in the peak positions or intensities were observed. (b) Contour plot of VTPXRD data collected on ZIF-zni, plotted between 14.2-15.8° 2θ. Subtle changes in the peak positions were observed with increasing temperature in accordance with their lattice parameter dependence. Changes in unit cell volume (c) and lattice parameters (d) during heating. Values obtained from Rietveld refinement of the variable temperature diffraction data at each temperature. The *a* lattice parameter increases with heating whilst the *c* parameter decreases with heating. The unit cell volume increases linearly from room temperature to *ca.* 350 °C at which temperature it deviates from this trend. This correlates with the feature seen in the DSC at *ca.* 360 °C. Changes in V/V$_0$ (e) revealed a 1.5% increase in unit cell volume occurred during heating. Changes in the available void space as a function of temperature (f) followed the same trends as the unit cell volume data and were calculated using Crystal Maker® X Version 10.5.4. It should be noted that the data collected at 450 °C have not been plotted as the uncertainty in the parameters was too great for the results to be meaningful.

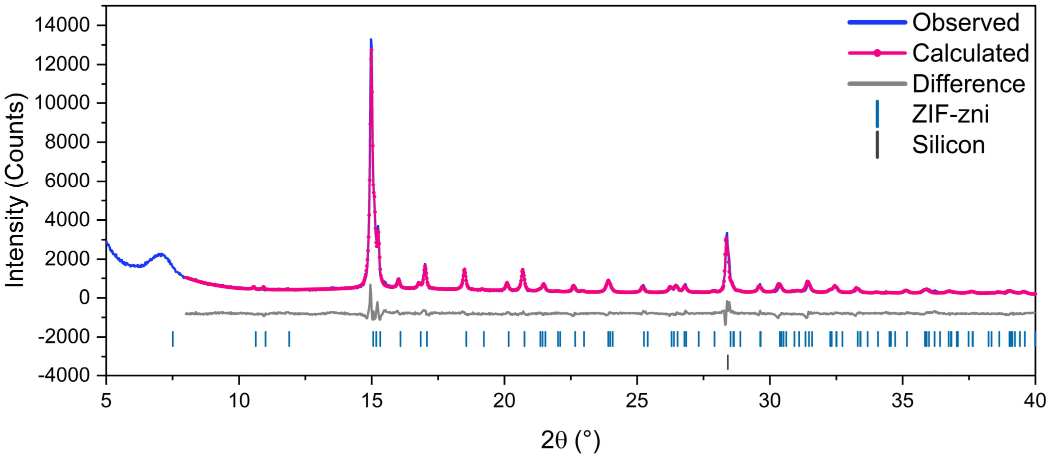

Figure S16: Example Rietveld refinement of the PXRD data collected for ZIF-zni at 30 °C. Simulated reflections for ZIF-zni are taken from a previously reported CIF.[3] Observed data (blue), calculated pattern (pink) and difference curve (grey) with simulated reflections of ZIF-zni (blue dashes) and silicon (grey dashes). Difference curve and Bragg positions are offset on the y axis for clarity.

Table S3: Data from Rietveld refinement of ZIF-zni at 30 °C

R_{wp}	Space Group	Lattice Parameters	Reported Parameters for ZIF-zni[3]
9.579	$I4_1cd$	a = 23.520(2) Å	a = 23.5028(4) Å
		c = 12.4626(15) Å	c = 12.4607(3) Å
		α = β = γ = 90 °	α = β = γ = 90 °

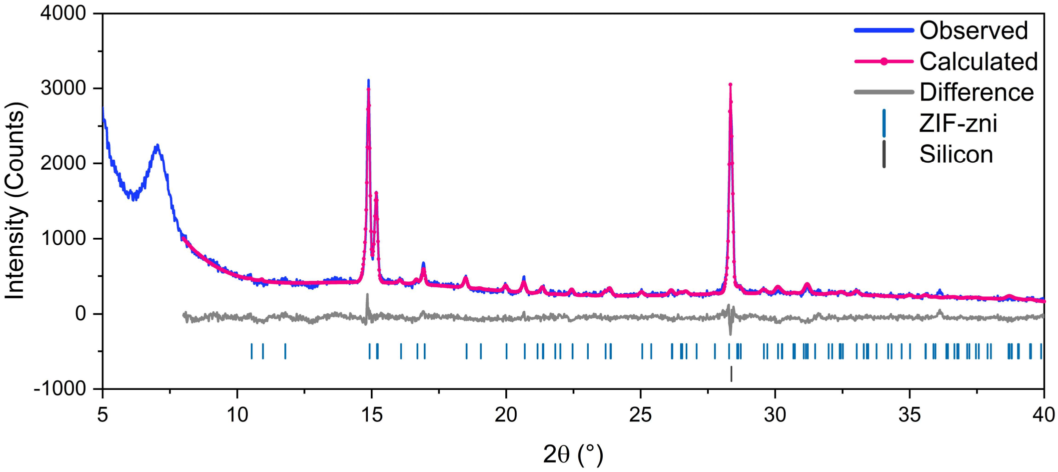

Figure S17: Example Rietveld refinement of the PXRD data collected for ZIF-zni at 430 °C. Simulated reflections for ZIF-zni are taken from a previously reported CIF.[3] Observed data (blue), calculated pattern (pink) and difference curve (grey) with simulated reflections of ZIF-zni (blue dashes) and silicon (grey dashes). Difference curve and Bragg positions are offset on the y axis for clarity.

Table S4: Data from Rietveld refinement of ZIF-zni at 430 °C

R_{wp}	Space Group	Lattice Parameters	Reported Parameters for ZIF-zni[3]
7.503	$I4_1cd$	a = 23.725(5) Å	a = 23.5028(4) Å
		c = 12.423(3) Å	c = 12.4607(3) Å
		α = β = γ = 90 °	α = β = γ = 90 °

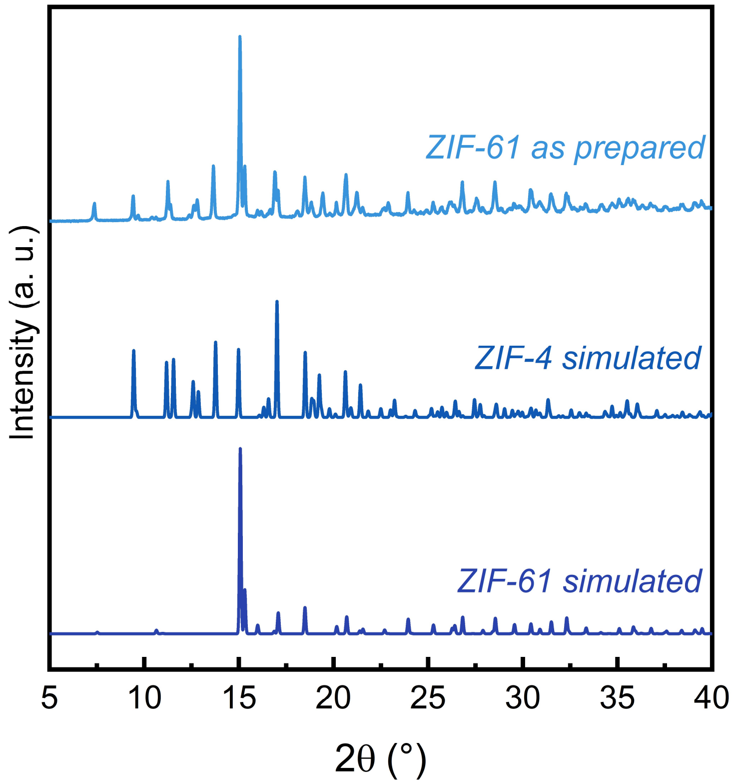

Figure S18: PXRD patterns between 5-40° of as prepared ZIF-61 (light blue) compared to the simulated diffraction pattern of ZIF-61 (dark blue) and ZIF-4 (mid-blue) obtained from previously published CIFs.[8,9] As prepared ZIF-61 was a mixed phase material containing reflections corresponding to both ZIF-61 and ZIF-4.

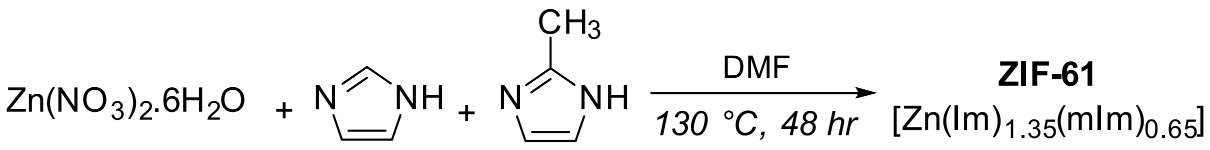

Figure S19: Reaction scheme for the optimised synthesis of ZIF-61.

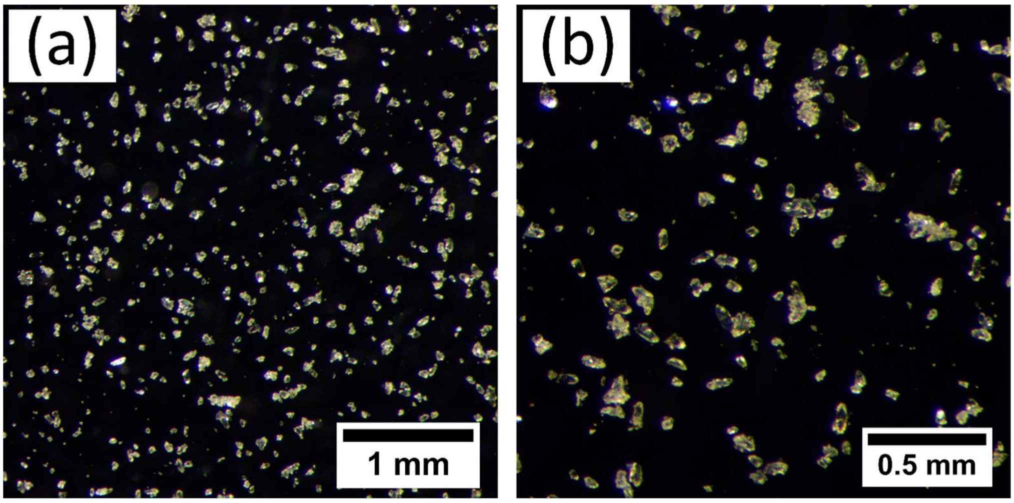

Figure S20: Optical microscope images of phase pure ZIF-61 crystals.

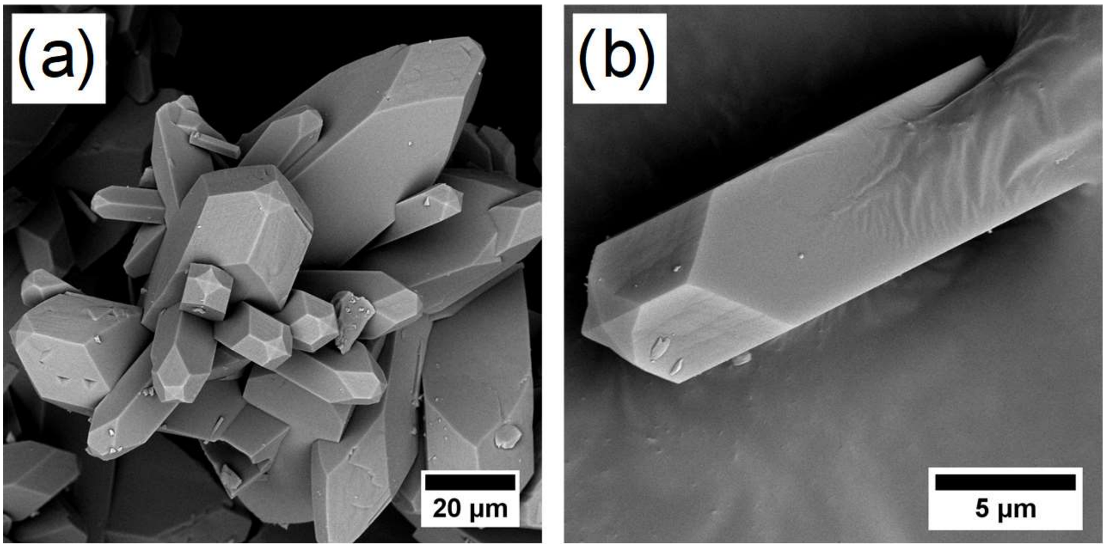

Figure S21: Scanning electron microscope images of phase pure ZIF-61 crystals.

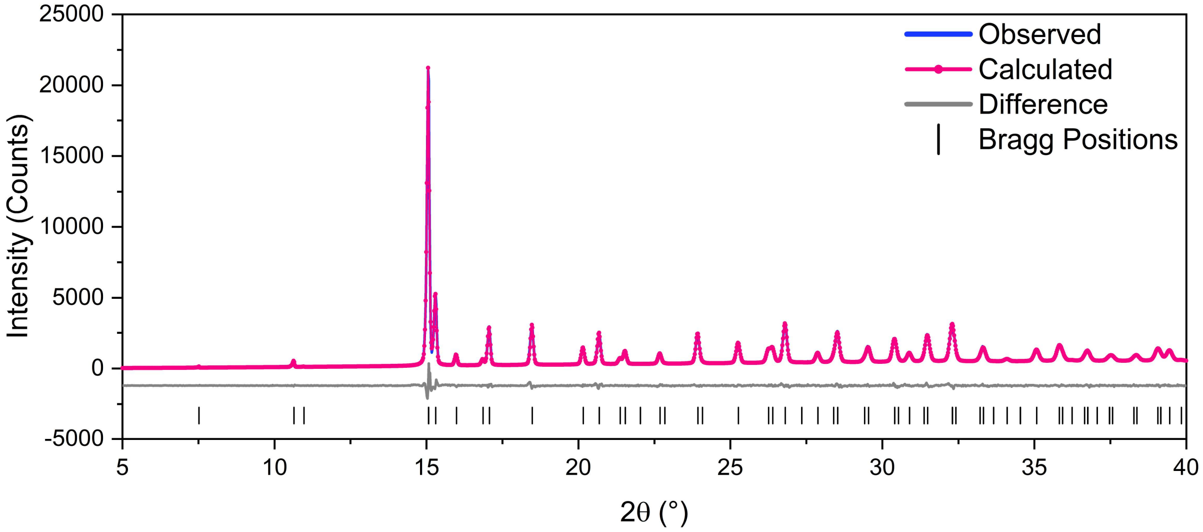

Figure S22: Pawley refinement of PXRD data of activated ZIF-61 powder. Initial parameters were obtained from the reported CIF for ZIF-61.[8] Difference curve and Bragg positions are offset on the y axis for clarity.

Table S5: Data from Pawley refinement of ZIF-61

R_{wp}	Space Group	Lattice Parameters	Reported Parameters for ZIF-61[8]
6.046	$I4_1acd$	a = 23.4965(8) Å c = 12.5606(7) Å α = β = γ = 90 °	a = 23.4803(3) Å c = 12.5545(3) Å α = β = γ = 90 °

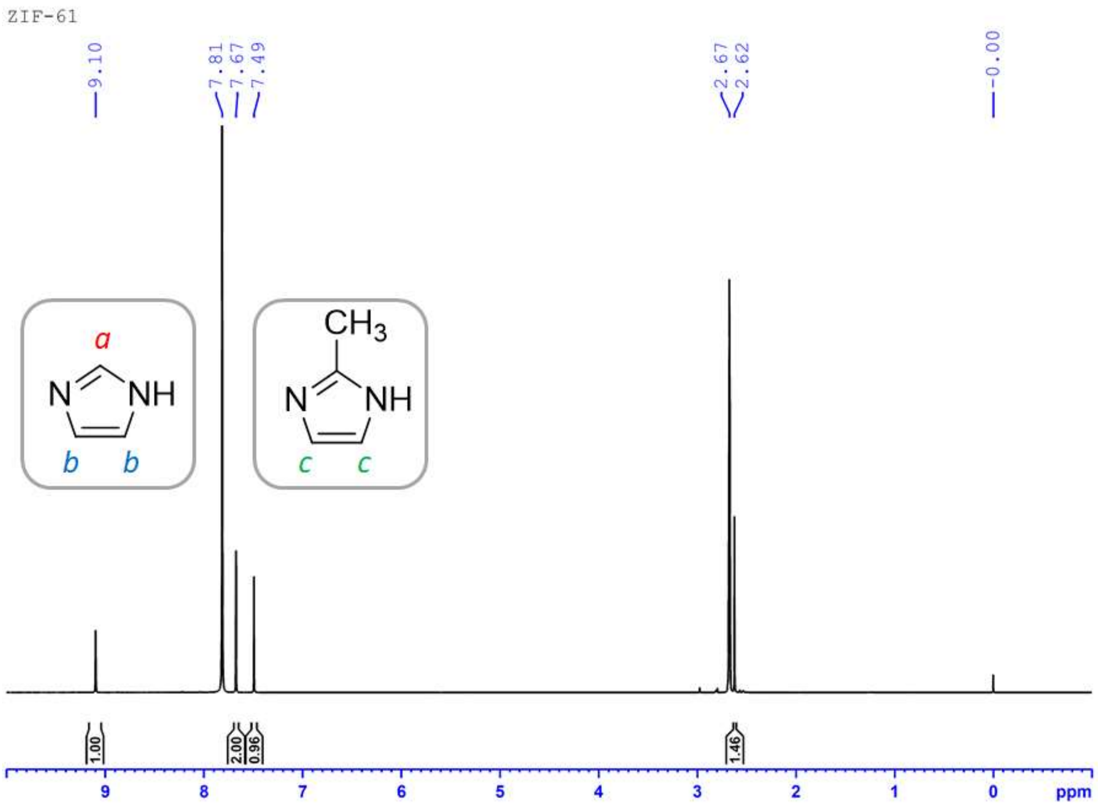

Figure S23: ^{1}H nuclear magnetic resonance (NMR) spectrum of ZIF-61. All analysis was performed using Topspin Version 4.0.7.[10] δH (500 MHz; DCl(35%)/D_2O:DMSO-d_6 (1:5); Me_4Si) 9.10 (1H, s, H*a*), 7.81 (H_2O/HCl), 7.67 (2H, s, H*b*), 7.49 (2H, 2, H*c*), 2.67 (DMSO), 2.62 (3H, s, -CH_3) 0.00 (TMS).

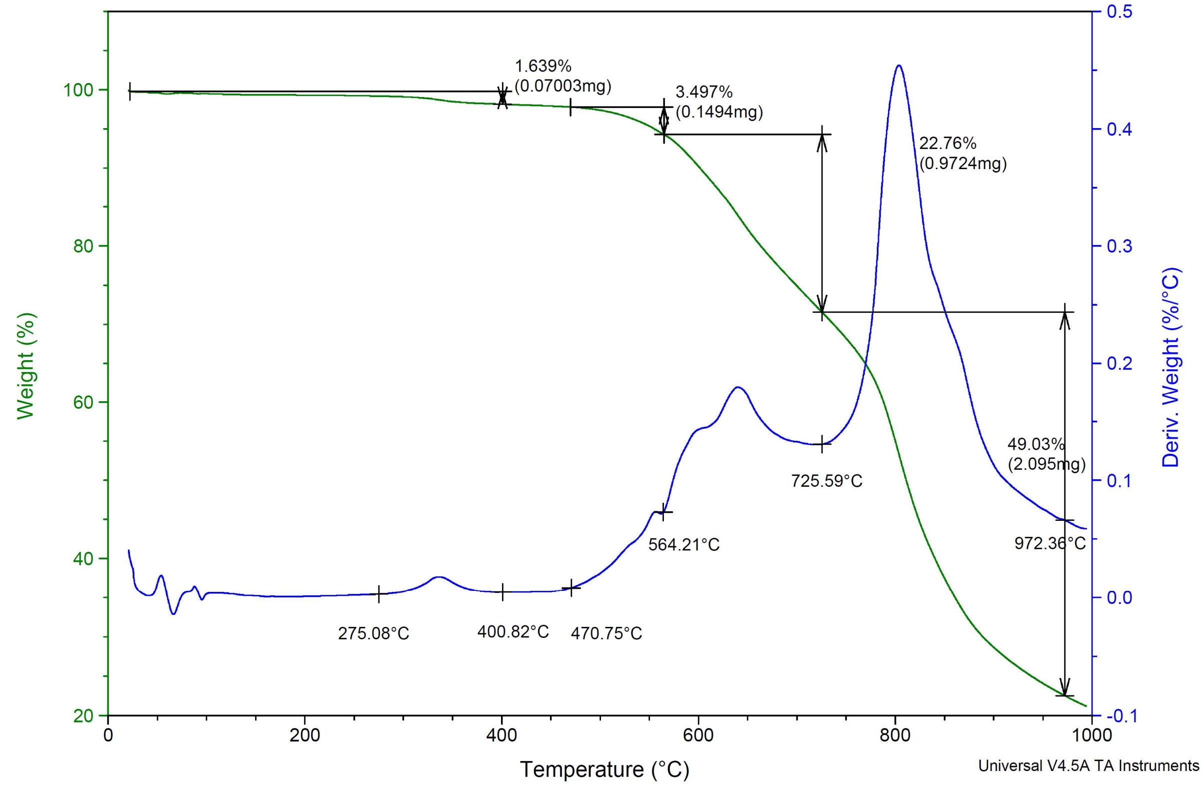

Figure S24: TGA of ZIF-61 powder heated at 10 °C min^{-1} up to 1000 °C under argon. Weight (%) curve shown in green and derivative weight (%/°C) curve shown in blue.

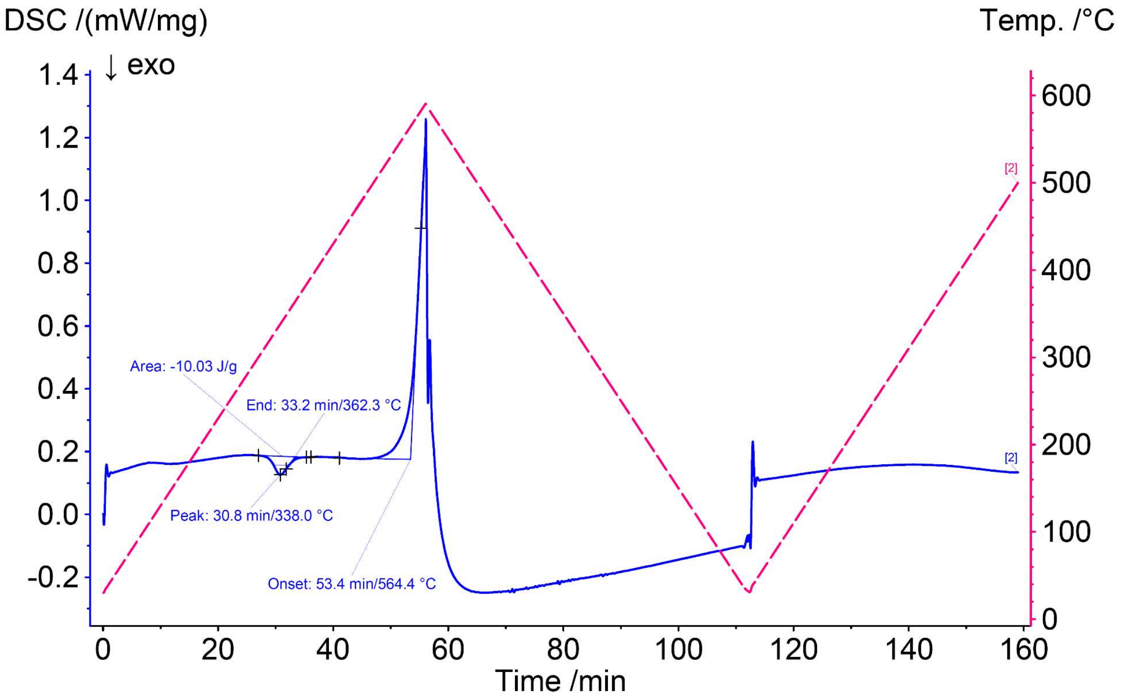

Figure S25: DSC of ZIF-61 powder heated to 590 °C, cooled to 30 °C and heated to 500 °C at 10 °C min^{-1} under argon. DSC curve shown in blue and temperature trace shown in pink. Unlike for ZIF-zni, the endotherm beginning at 564 °C, did not reach its peak before the end of the first upscan. As this event is highly energetic and there was no visible T_g in the second upscan, this event is ascribed to decomposition, rather than melting.

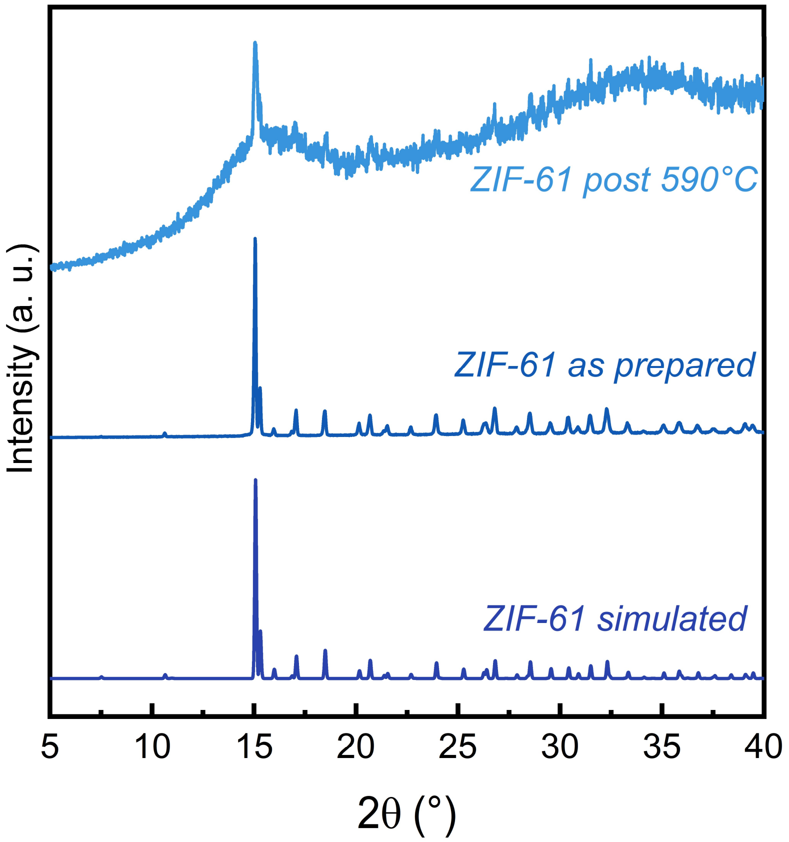

Figure S26: PXRD patterns between 5-40° of as prepared ZIF-61 (mid-blue) and ZIF-61 after 590 °C (light blue) compared to the simulated diffraction pattern of ZIF-61 (dark blue) obtained from previously published CIF.[8] After heating to 590 °C, ZIF-61 still exhibited Bragg reflections corresponding to the ZIF-61 crystal structure, suggesting that decomposition, rather than melting had occurred.

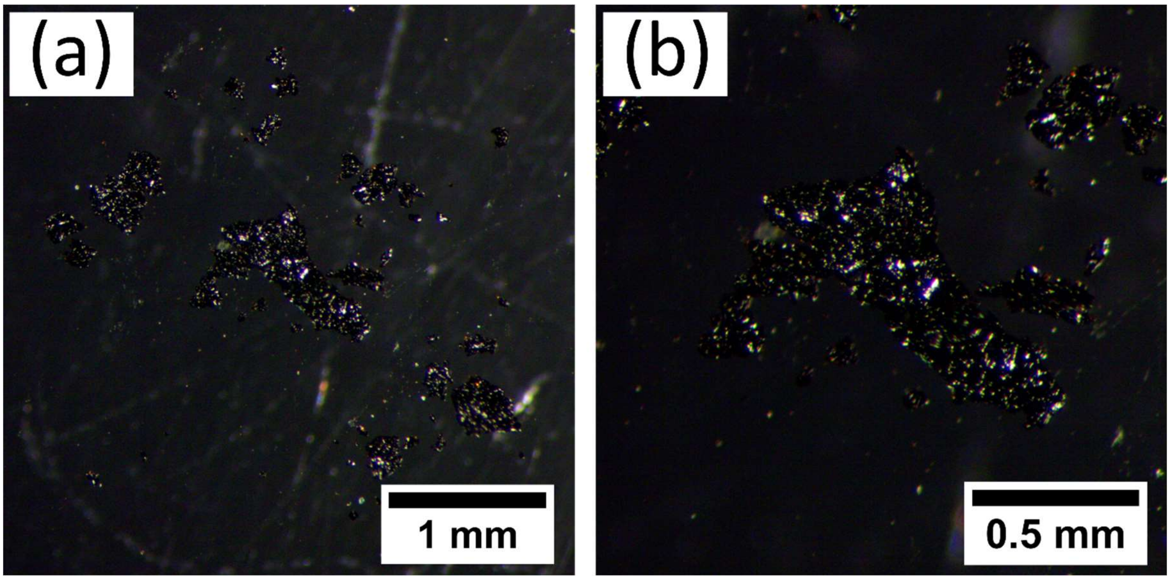

***Figure S27**:* Optical microscope images of ZIF-61 after heating to 590 °C. Significant sample decomposition was evident from the colour change from pale yellow to black. Some particle amalgamation had occurred but there was minimal evidence of flow into larger continuous pieces.

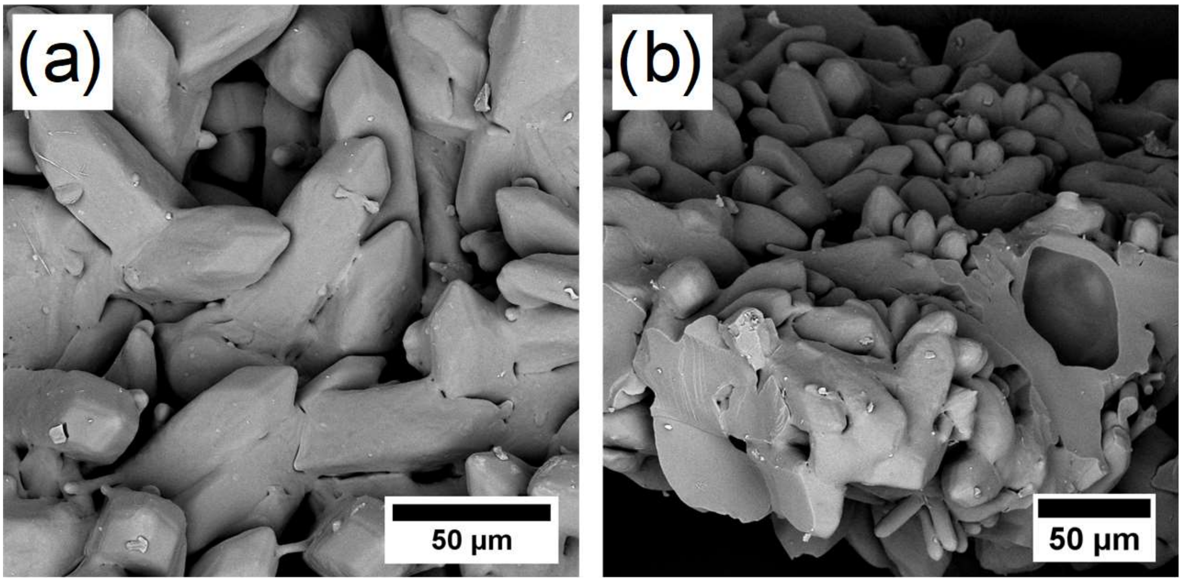

Figure S28: Scanning electron microscope images of ZIF-61 after heating to 590 °C. Some particle coalescence and bubble formation were evident. However, the facets of the original crystals were still visible, albeit more rounded in nature, thus supporting sample decomposition rather than glass formation.

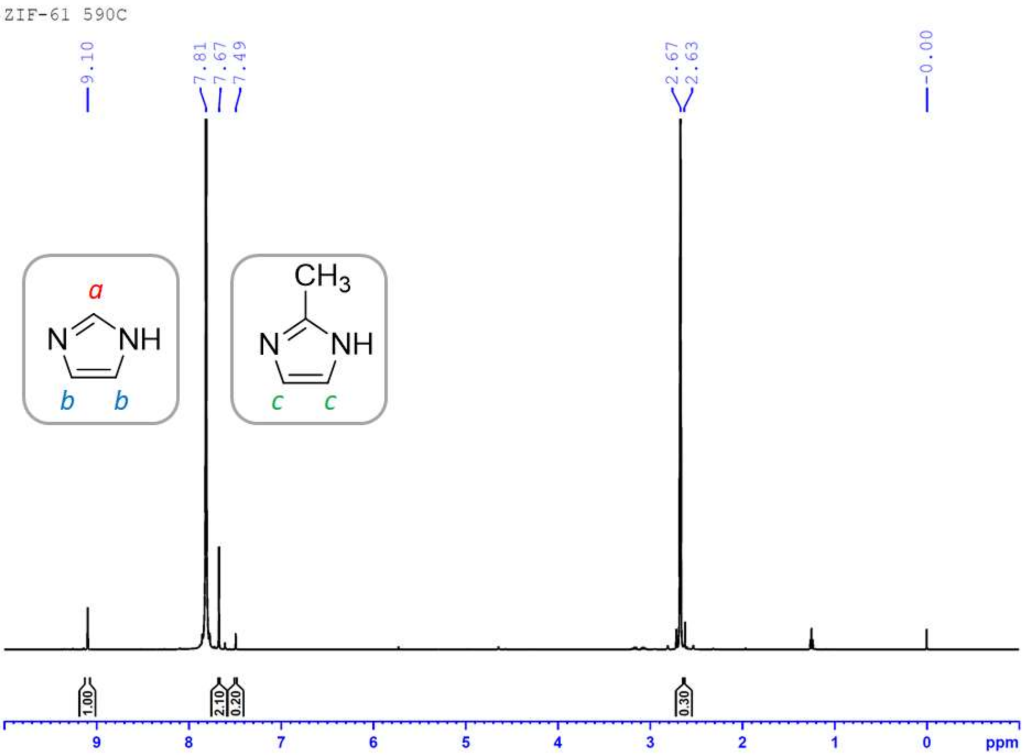

Figure S29: ^{1}H NMR spectrum of ZIF-61 after heating to 590 °C. δH (500 MHz; DCl(35%)/D_2O:DMSO-d_6 (1:5); Me_4Si) 9.10 (1H, s, H*a*), 7.81 (H_2O/HCl), 7.67 (2H, s, H*b*), 7.49 (2H, 2, H*c*), 2.67 (DMSO), 2.63 (3H, s, -CH_3) 0.00 (TMS).

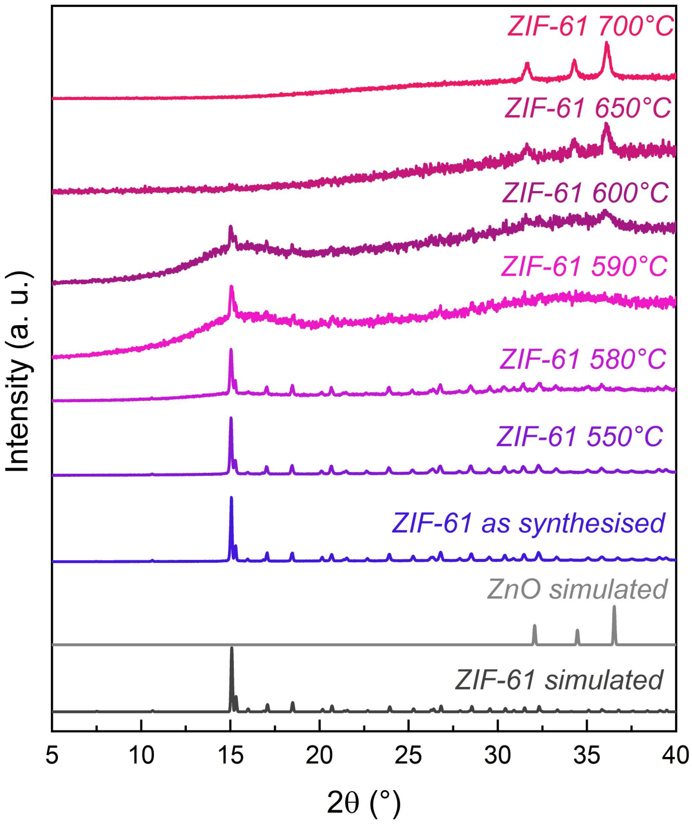

Figure S30: PXRD patterns between 5-40° of as prepared ZIF-61 (blue) and ZIF-61 heated to 550-700 °C (purple to red) compared to the simulated diffraction pattern of ZIF-61 (dark grey) and ZnO (light grey). Evidence of ZnO is observed at 600 °C, alongside reflections corresponding to ZIF-61. Above 650 °C, there is little evidence of diffuse scattering, only ZnO, suggesting decomposition has occurred without melting.

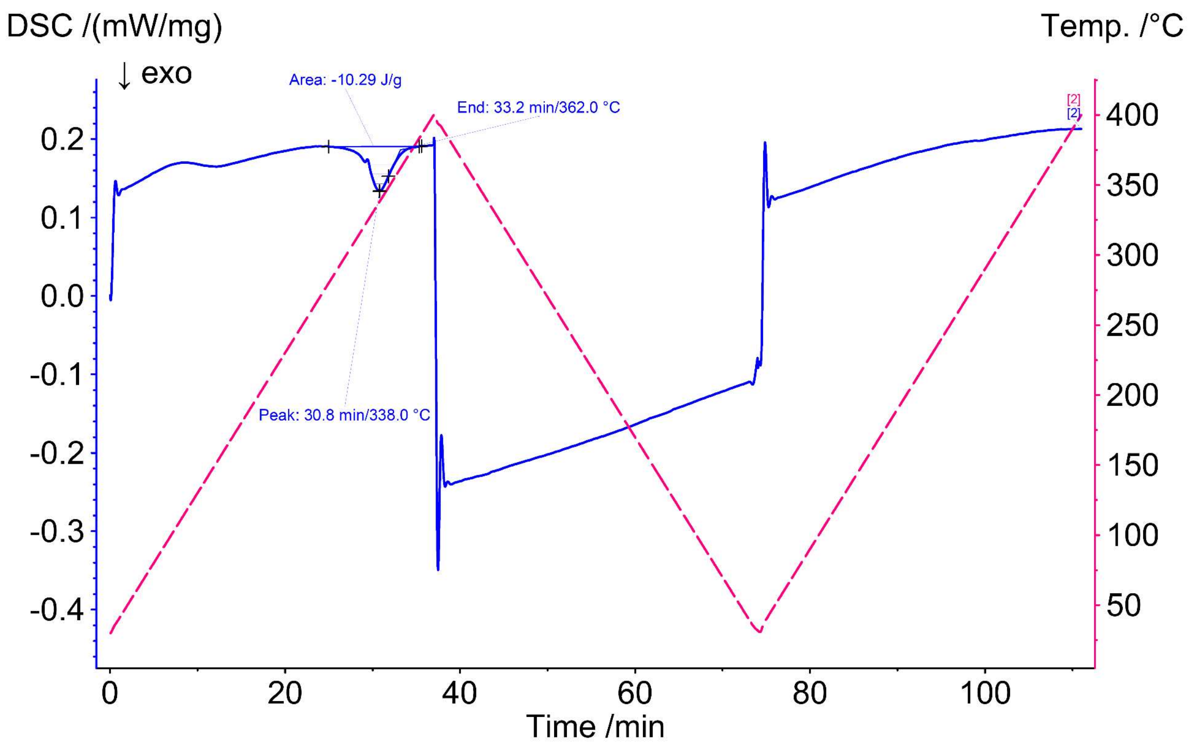

Figure S31: DSC of ZIF-61 powder heated to 400 °C, cooled to 30 °C and heated to 400 °C at 10 °C min^{-1} under argon. DSC curve shown in blue and temperature trace shown in pink. Time is shown on the x-axis.

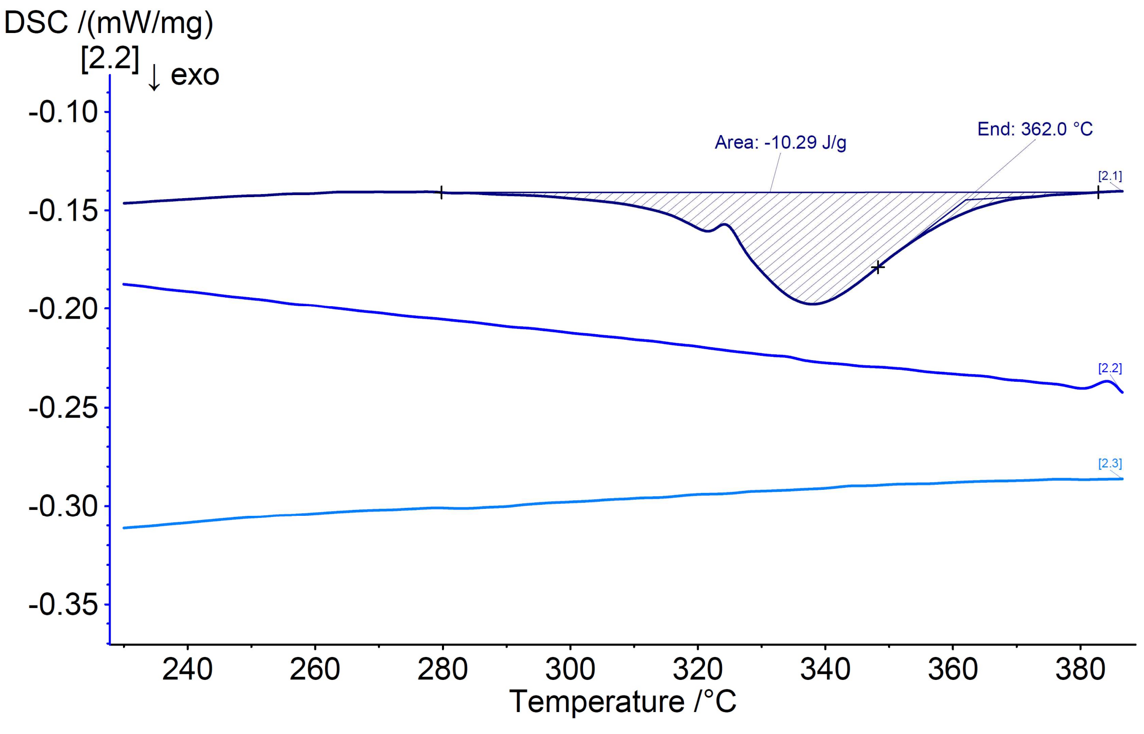

Figure S32: DSC of ZIF-61 powder heated to 400°C, cooled to 30°C and heated to 400°C at 10°C min^{-1} under argon. Temperature is shown on the x-axis. DSC traces are separated into segments: 1st upscan – navy, downscan – blue, 2nd upscan – light blue. DSC segments are offset on the y-axis for clarity.

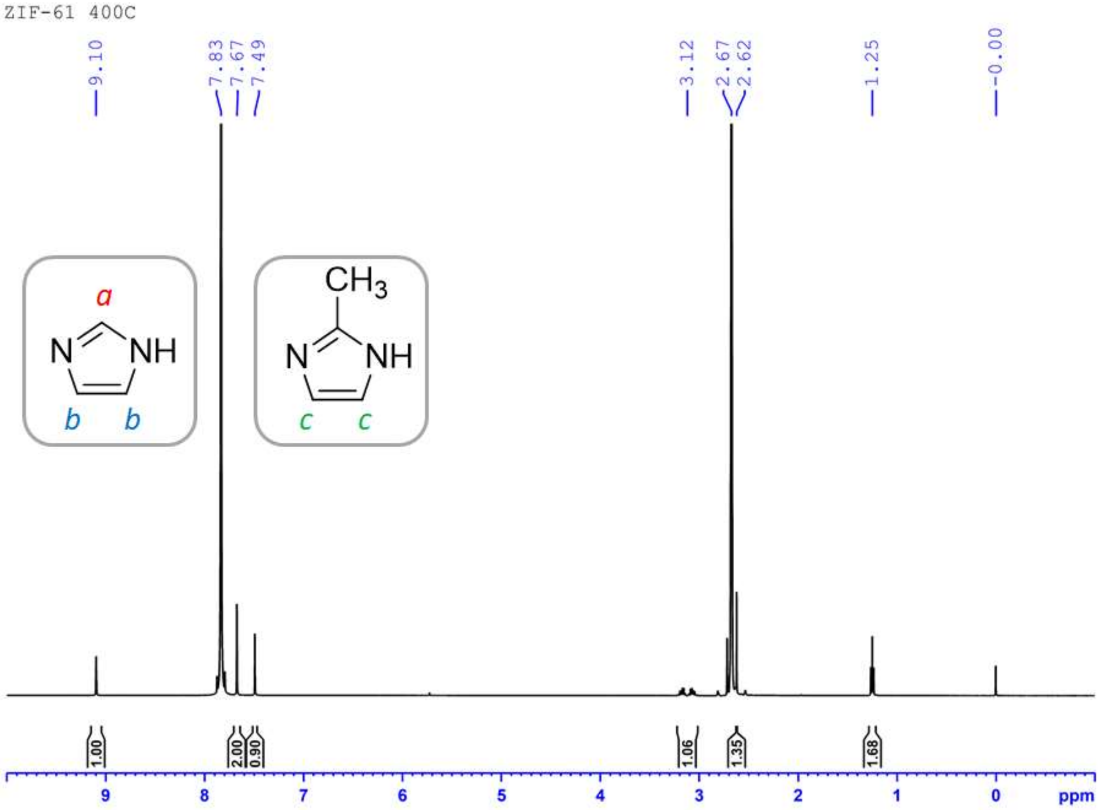

Figure S33: ^{1}H NMR spectrum of ZIF-61 after heating to 400 °C. δH (500 MHz; DCl(35%)/D_2O:DMSO-d_6 (1:5); Me_4Si) 9.10 (1H, s, H*a*), 7.83 (H_2O/HCl), 7.67 (2H, s, H*b*), 7.49 (2H, 2, H*c*), 2.67 (DMSO), 2.62 (3H, s, -CH_3) 0.00 (TMS).

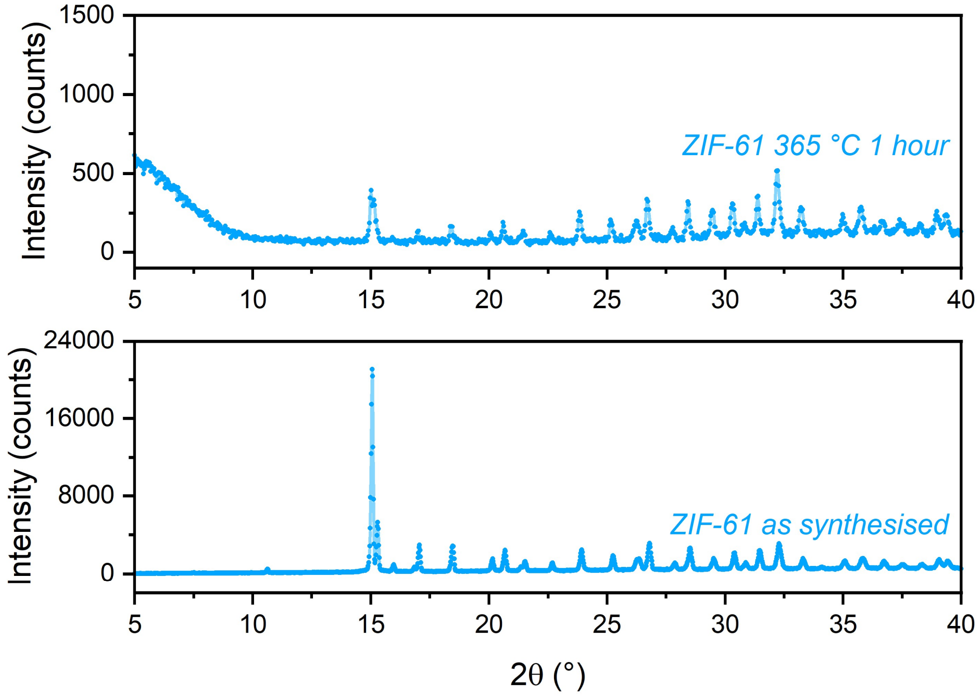

Figure S34: PXRD patterns between 5-40° of as prepared ZIF-61 (bottom pane) and ZIF-61 heated to 365 °C for 1 hour (top pane). No discernible difference in the number or position of reflections was observed, with the only noticeable change being a considerable drop in the overall intensity after heating.

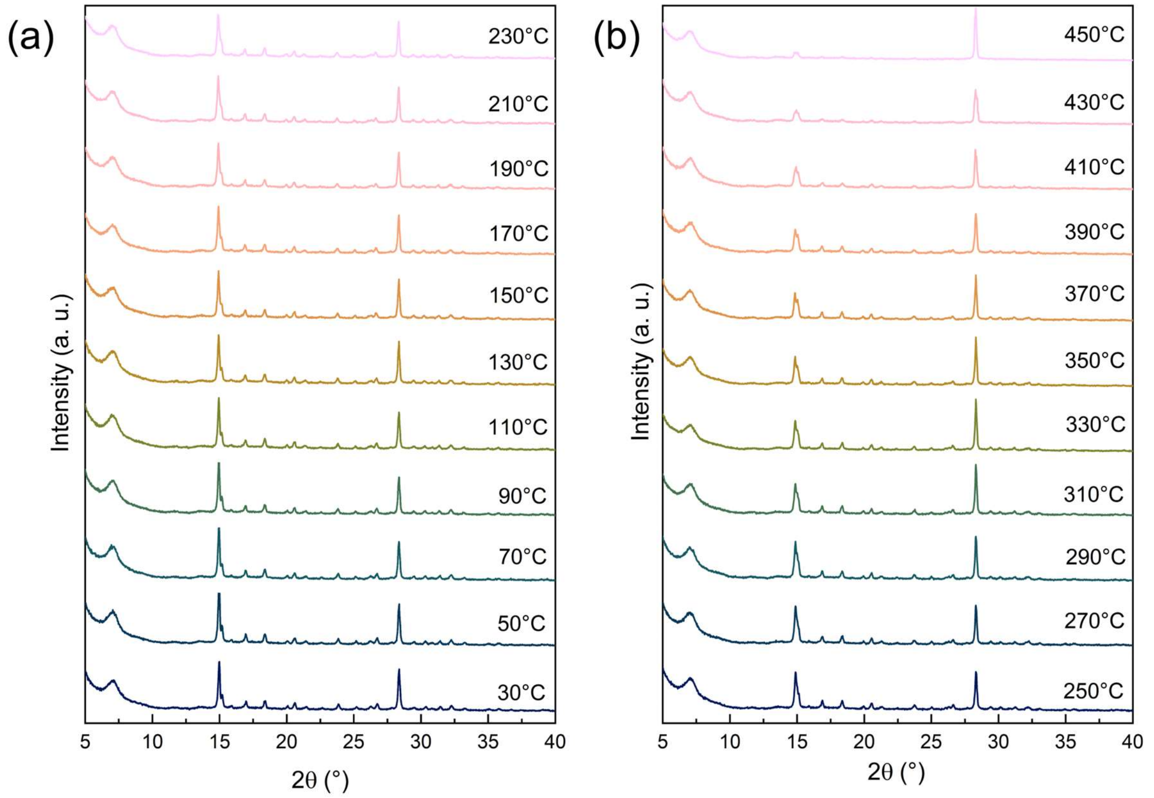

Figure S35: VTPXRD data for ZIF-61 between 30 and 230 °C (a) and 250 °C and 450 °C (b). Data were collected at 20 °C intervals from 30 °C to 450 °C and a silicon standard was used as a reference. Data quality reduces significantly above 250 °C and this is attributed to sample decomposition. The broad peak at 7° is from the alumina sample holder.

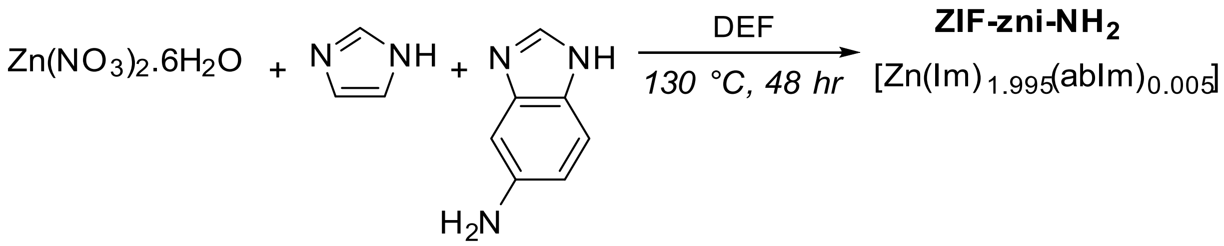

Figure S36: Reaction scheme for the synthesis of ZIF-zni-NH_2.

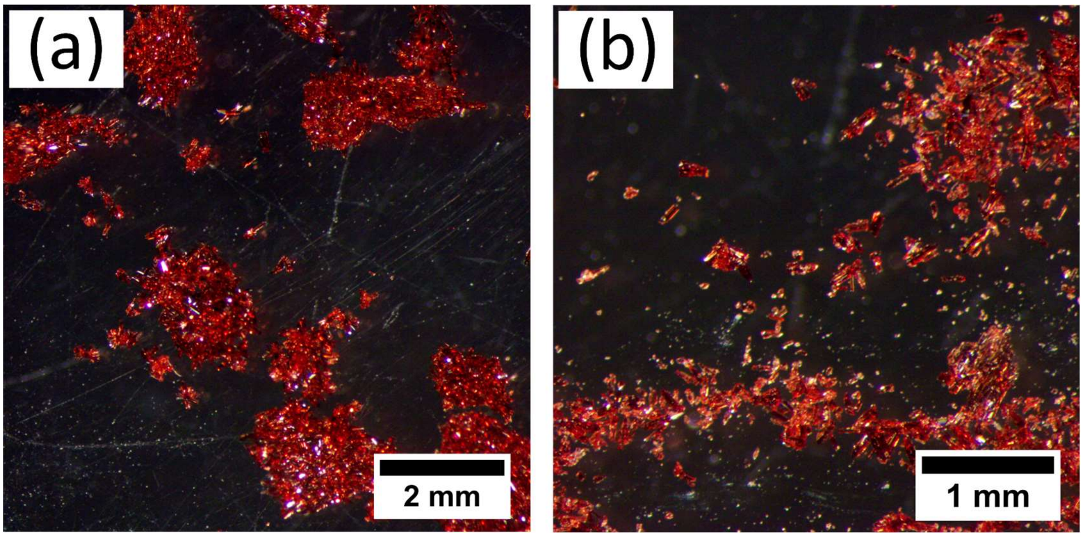

Figure S37: Optical microscope images of phase pure ZIF-zni-NH_2 crystals.

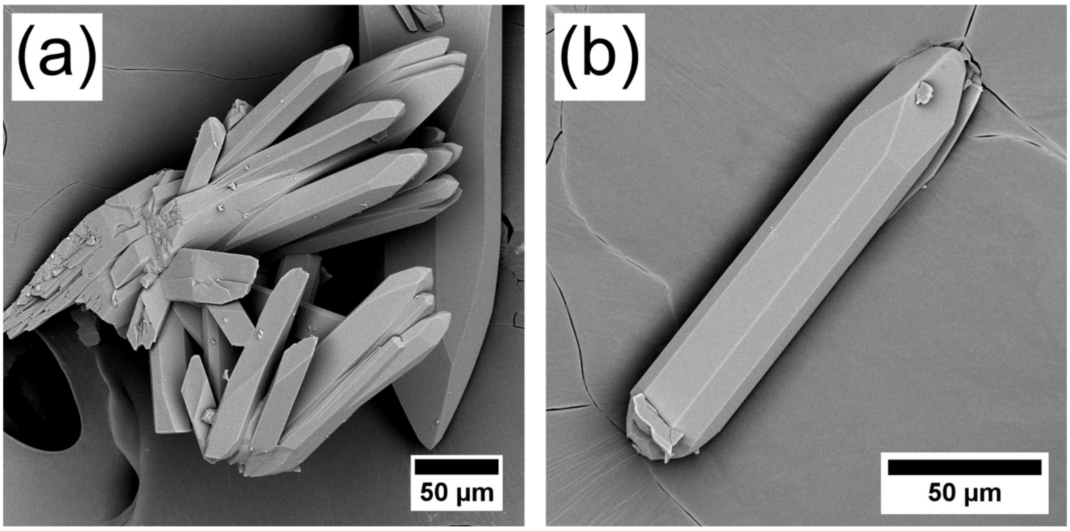

Figure S38: Scanning electron microscope images of phase pure ZIF-zni-NH_2 crystals.

Table S6: Data from Pawley refinement of ZIF-zni-NH_2

R_{wp}	Space Group	Lattice Parameters	Reported Parameters for ZIF-zni[3]
8.466	$I4_1cd$	a = 23.5097(3) Å	a = 23.5028(4) Å
		c = 12.4672(5) Å	c = 12.4607(3) Å
		α = β = γ = 90 °	α = β = γ = 90 °

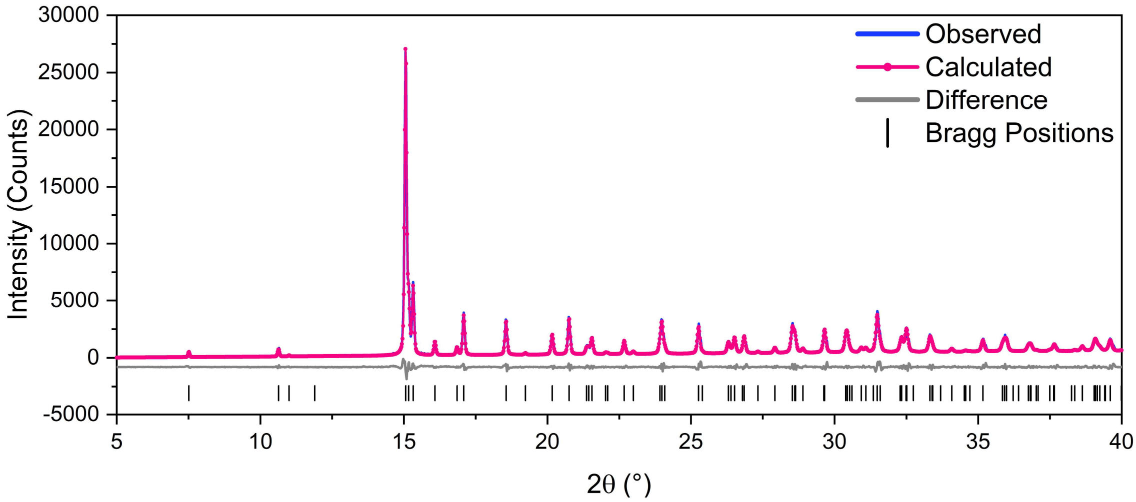

Figure S39: Pawley refinement of PXRD data of ZIF-zni-NH$_2$. Initial parameters were obtained from the reported CIF for ZIF-zni.[3] Difference curve and Bragg positions are offset on the y axis for clarity.

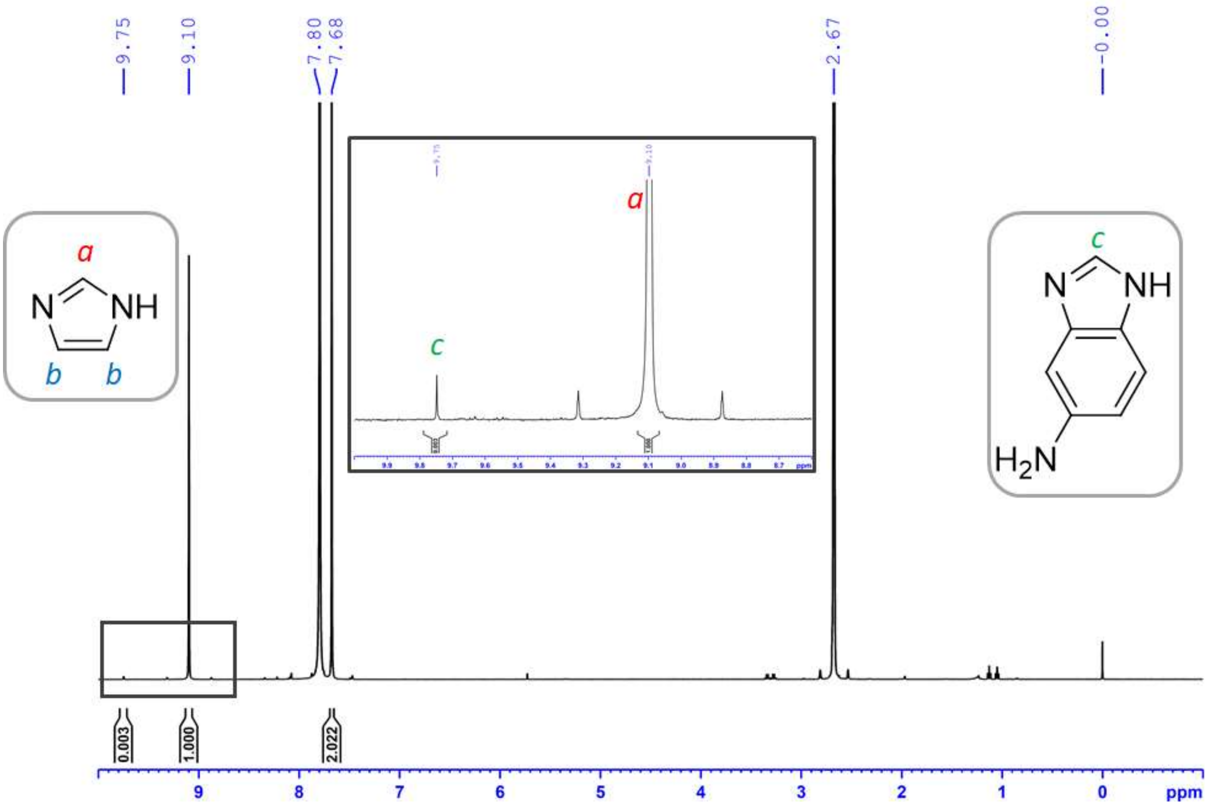

Figure S40: ^{1}H NMR spectrum of ZIF-zni-NH$_2$. δH (500 MHz; DCl(35%)/D_2O:DMSO-d_6 (1:5); Me_4Si) 9.75 (1H, s, H*c*), 9.10 (1H, s, H*a*), 7.80 (H_2O/HCl), 7.68 (2H, s, H*b*), 2.67 (DMSO), 0.00 (TMS).

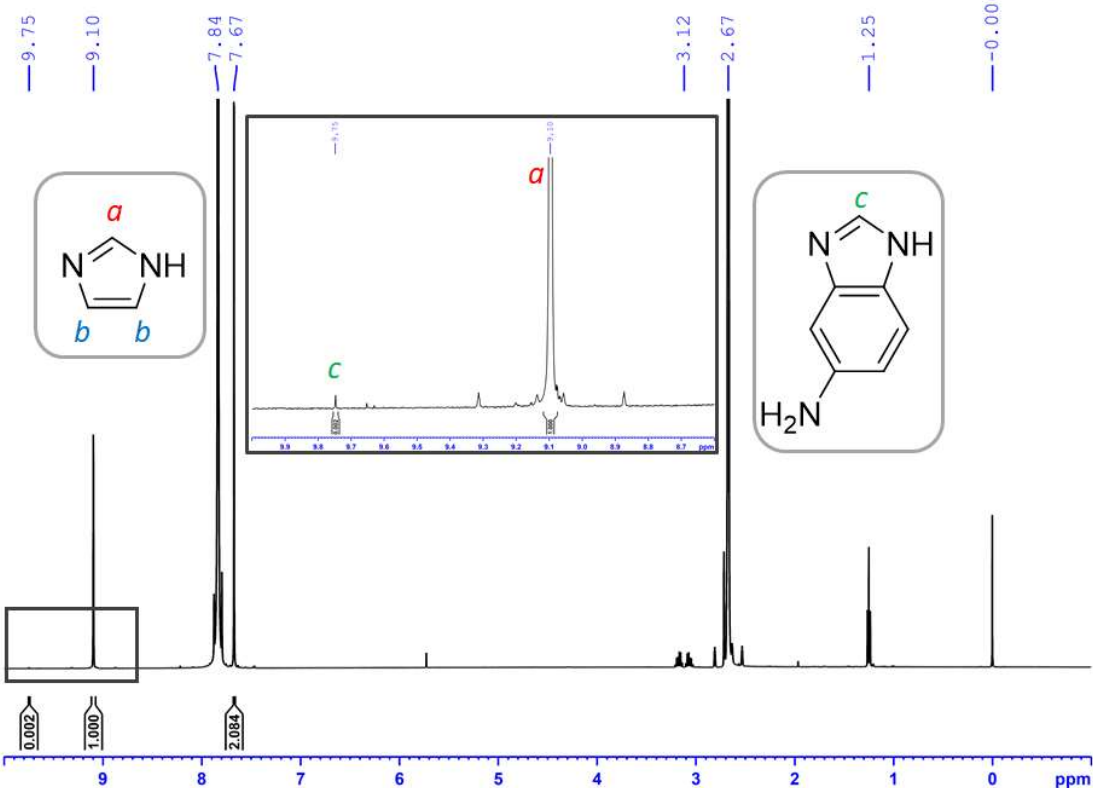

Figure S41: ^{1}H NMR spectrum of ZIF-zni-NH_2 after heating to 400 °C. All analysis was performed using Topspin Version 4.0.7.[10] δH (500 MHz; DCl(35%)/D_2O:DMSO-d_6 (1:5); Me_4Si) 9.75 (1H, s, Hc), 9.10 (1H, s, Ha), 7.84 (H_2O/HCl), 7.67 (2H, s, Hb), 2.67 (DMSO), 0.00 (TMS).

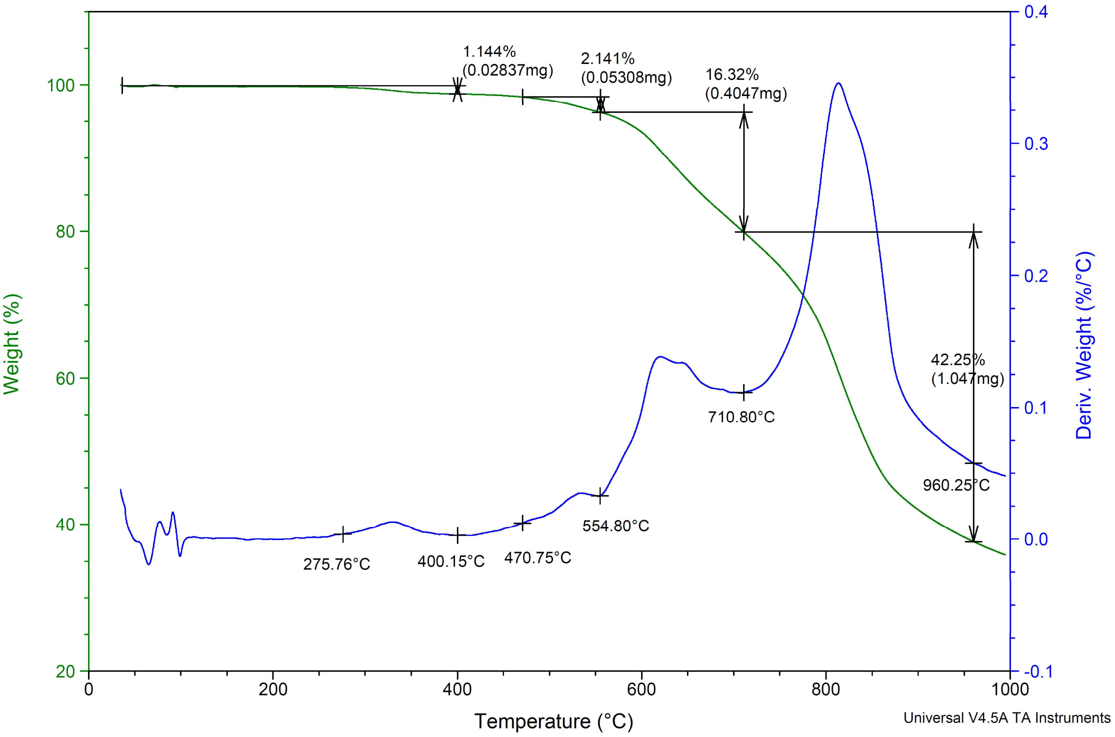

Figure S42: TGA of ZIF-zni-NH_2 powder heated at 10 °C min^{-1} up to 1000 °C under argon. Weight (%) curve shown in green and derivative weight (%/°C) curve shown in blue.

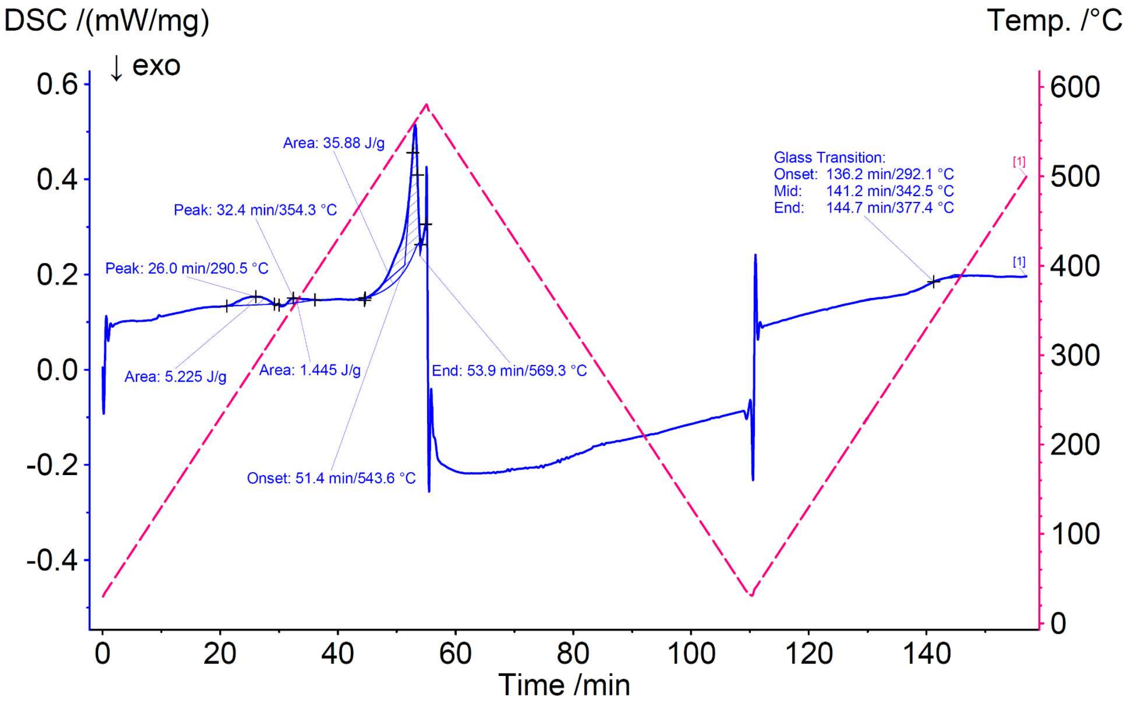

Figure S43: DSC of ZIF-zni-NH$_2$ powder heated to 580 °C, cooled to 30 °C and heated to 500 °C at 10 °C min^{-1} under argon. DSC curve shown in blue and temperature trace shown in pink.

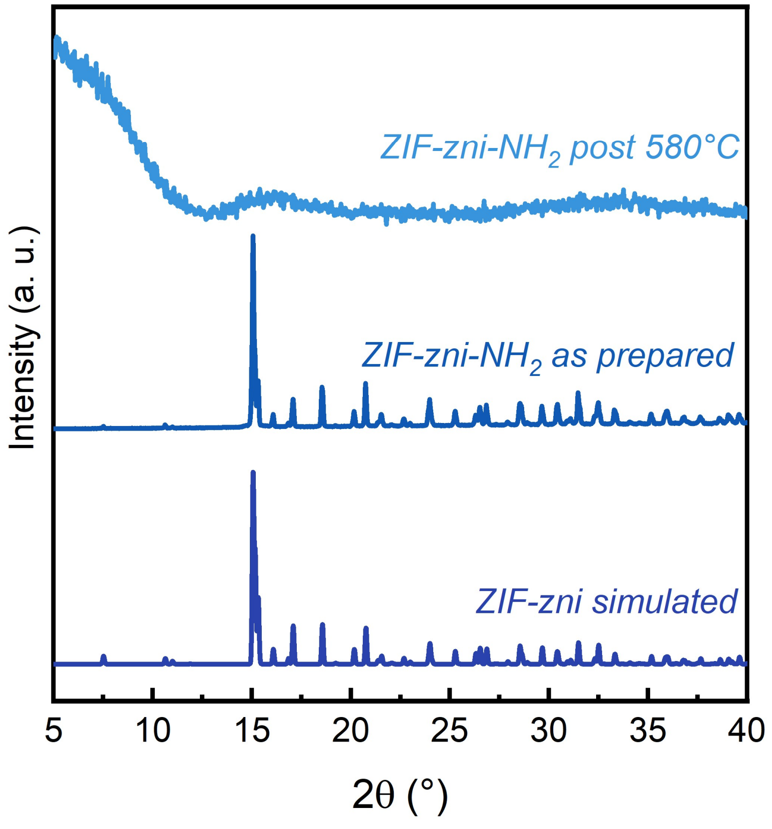

Figure S44: PXRD patterns between 5-40° of as prepared ZIF-zni-NH$_2$ (mid blue) and a_g ZIF-zni-NH$_2$ (light blue) (after heating to 580 °C) compared to the simulated diffraction pattern of ZIF-zni (dark blue) obtained from previously published CIF[3].

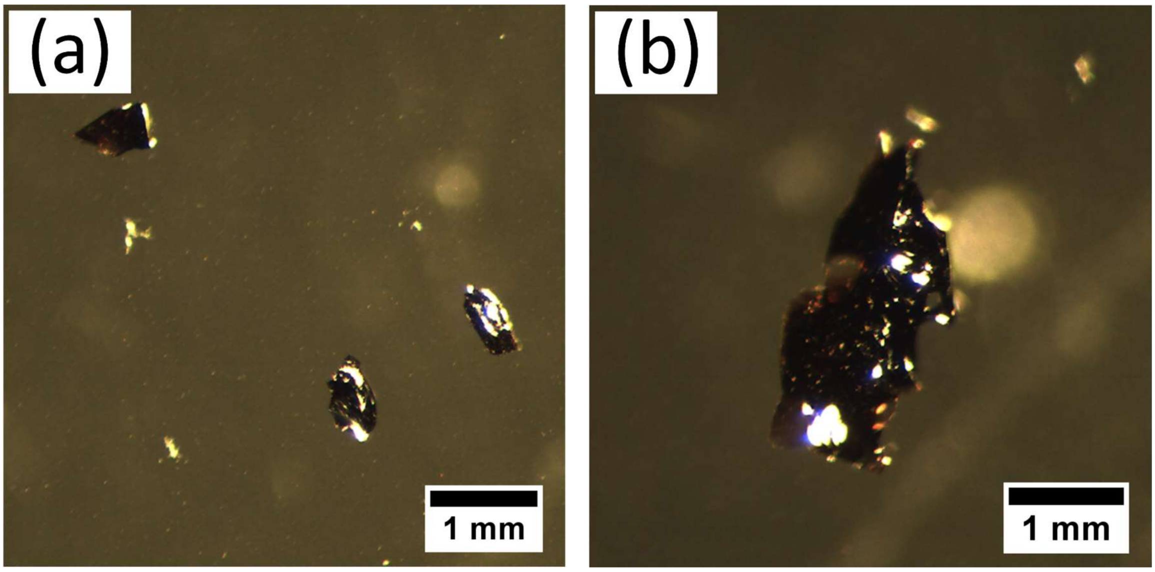

Figure S45: Optical microscope images of ZIF-zni-NH$_2$ after heating to 580 °C. Clear evidence of flow and glass formation had occurred, although decomposition related discolouration was also observed.

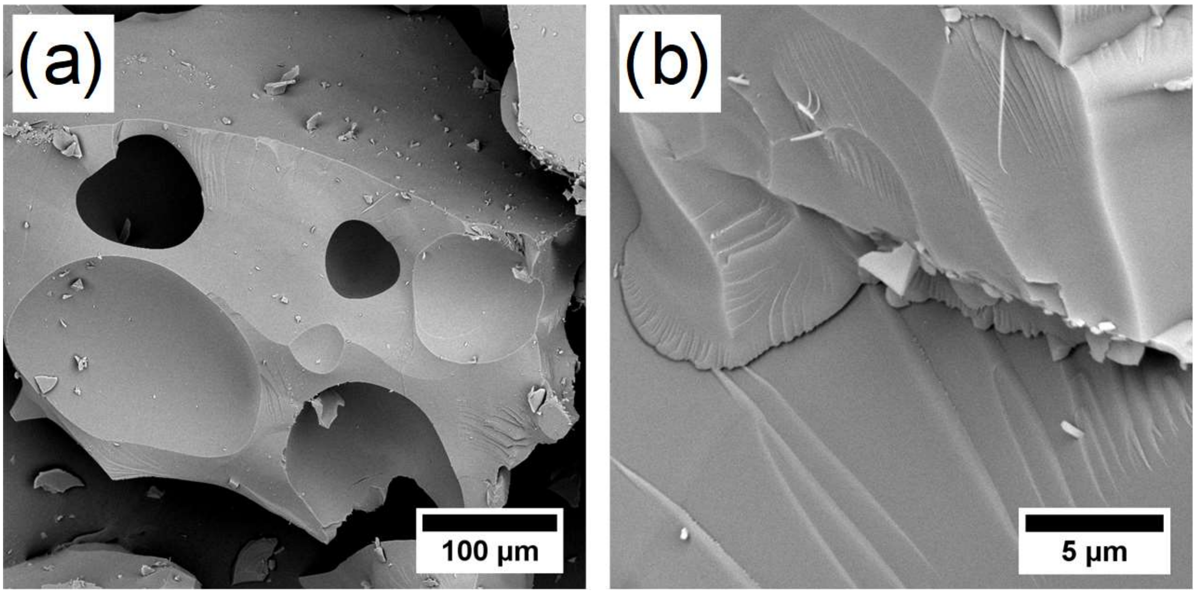

Figure S46: Scanning electron microscope images of ZIF-zni-NH$_2$ after heating to 580 °C. Clear evidence of flow related striations and bubbles were visible, supporting that glass formation had occurred.

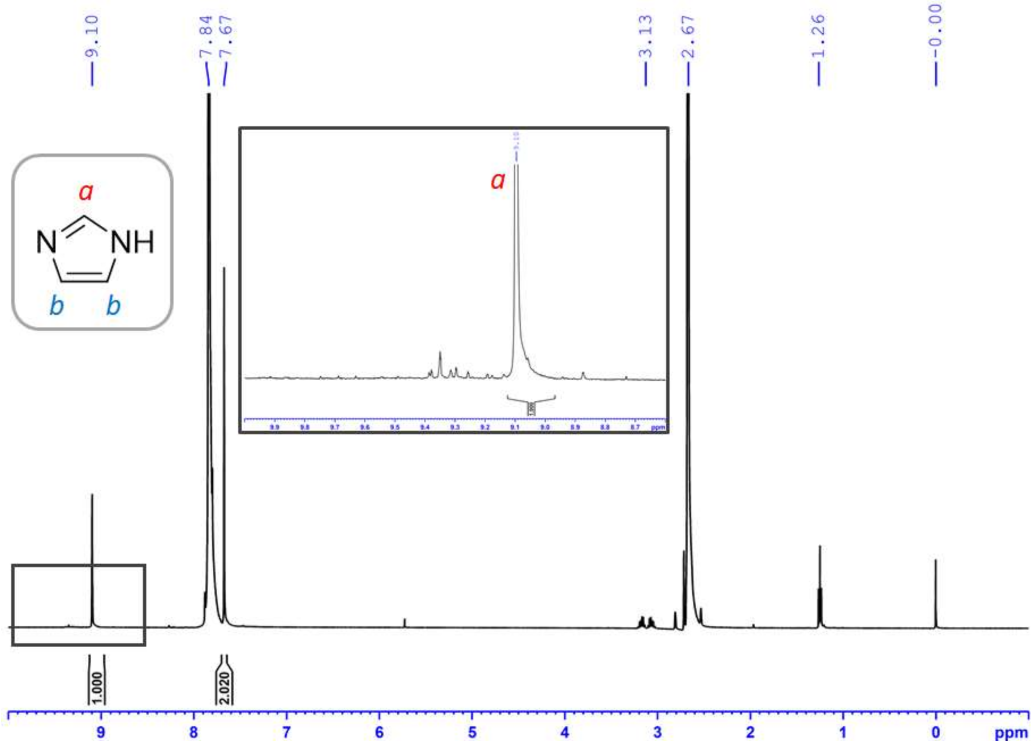

Figure S47: ^{1}H NMR spectrum of ZIF-zni-NH_2 after heating to 580 °C. δH (500 MHz; DCl(35%)/D_2O:DMSO-d_6 (1:5); Me_4Si) 10.0-8.6 (unknown decomposition products), 9.10 (1H, s, H*a*), 7.84 (H_2O/HCl), 7.67 (2H, s, H*b*), 2.67 (DMSO), 0.00 (TMS).

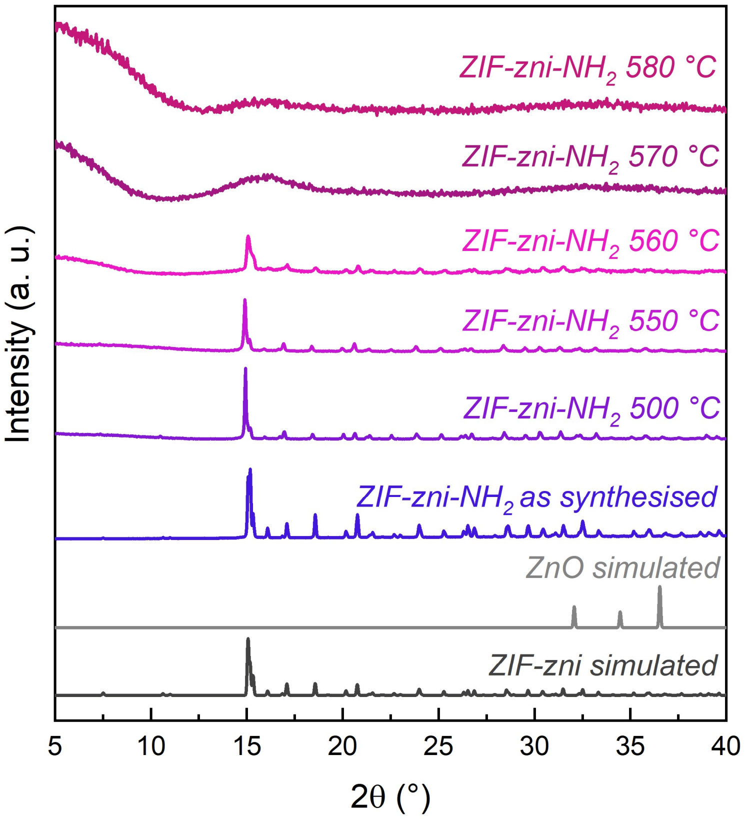

***Figure S48**:* PXRD patterns between 5-40° of as prepared ZIF-zni-NH_2 (blue) and ZIF-zni-NH_2 heated to 500-580 °C (purple to red) compared to the simulated diffraction pattern of ZIF-zni (dark grey) and ZnO (light grey). Only diffuse scattering was observed for a_gZIF-zni-NH_2 at 570 °C or 580 °C and there was no evidence of decomposition to ZnO at high temperatures.

References

1 D. M. Schubert, M. Z. Visi and C. B. Knobler, *Main Group Chem.*, 2008, **7**, 311–322.

2 C. A. Schneider, W. S. Rasband and K. W. Eliceiri, *Nat. Methods*, 2012, **9**, 671–675.

3 E. C. Spencer, R. J. Angel, N. L. Ross, B. E. Hanson and J. A. K. Howard, *J. Am. Chem. Soc.*, 2009, **131**, 4022–4026.

4 N. Kourkoumelis, in *ICDD Annual Spring Meetings*, ed. L. O'Neill, Cambridge University Press, Cambridge, 2013, pp. 137–148.

5 A. A. Coelho, *J. Appl. Crystallogr.*, 2018, **51**, 210–218.

6 UNIVERSAL ANALYSIS 2000 (Version 4.5A), TA Instruments, New Castle, Delaware, 2000.

7 PROTEUS (Version 8.0.2), Netzsch, Selb, Germany, 2020.

8 R. Banerjee, A. Phan, B. Wang, C. Knobler, H. Furukawa, M. O'Keeffe and O. M. Yaghi, *Science*, 2008, **319**, 939–943.

9 K. S. Park, Z. Ni, A. P. Cote, J. Y. Choi, R. Huang, F. J. Uribe-Romo, H. K. Chae, M. O'Keeffe and O. M. Yaghi, *Proc. Natl. Acad. Sci.*, 2006, **103**, 10186–10191.

10 TOPSPIN (Version 4.0.7), Bruker, Billerica, Massachusetts, 2019.